

Towards formalization of the soliton counting technique for the Khovanov–Rozansky invariants by means of the deformed \mathcal{R} -matrix approach

A. Anokhina*

Abstract

We attempt to consider the recently developed Cohomological field theory soliton counting diagram technique for the Khovanov and Khovanov–Rozansky invariants [1, 2]. Although the hope to obtain a new way for computing the invariants did not yet come true, we demonstrate that soliton counting technique can be totally formalized at an intermediate stage, at least in the particular cases. We present in details the corresponding algorithm, based on the deformed \mathcal{R} -matrix and minimal positive division approach, earlier developed by ourselves [3]. We start from a detailed review of the latter approach, comparing it with different ones, including the strict mathematical treatment [4]. Examples of data that can be obtained in the suggested way are presented in the Appendices.

Contents

1	Introduction	2
1.1	Different approaches to KhR invariants	4
1.2	Conjectures and hopes	4
2	A sketch of the general construction	4
2.1	The initial set	4
2.2	The explicit expression for the knot invariants	7
2.3	The resolution hypercube	8
2.4	Vector spaces at the hypercube vertices	10
2.5	Spaces at vertices as graded spaces	11
2.6	From the resolution hypercube to the complex	12
2.7	Graded basis in the homologies	13
2.8	The geometric sense of the “positive integer” decomposition	14
3	A minimal positive division instead of computing the homology	14
3.1	General definitions	14
3.1.1	Complex, homologies and decomposition of the generating functions.	14
3.1.2	Integer and polynomial division.	15
3.1.3	Division as computing homology	16
3.2	“Ambigiuos” and “anambigiuos” minimal remainders	17
3.3	Properties of maps as “selection rules” for the “minimal remainder”	17
3.3.1	Ranks of the differentials	17
3.3.2	Particular values of matrix elements	18
3.4	“Multilevel” division as a way to fix ambiguities	19

*ITEP, Moscow, Russia; anokhina@itep.ru

4 Lie algebra structure in the complex and its breaking	19
4.1 Spaces in the resolution hypercube as representation spaces	20
4.2 Are the homology spaces representation spaces?	20
4.2.1 A toy example	21
4.2.2 Relation to the real case	21
4.3 Differential expansion and evolution method	22
4.3.1 Schematic sketch of the approaches	22
4.3.2 An interplay with positive division method	22
5 Minimal positive division approach and the CohFT calculus	23
5.1 Preliminary comments	23
5.1.1 CohFT diagram technique	23
5.1.2 The selection rule for the CohFT matrix elements	23
5.1.3 Types of the CohFT matrix elements and multilevel division	23
5.1.4 Our program	24
5.2 Division algorithm for a generic two strand knot	24
5.2.1 The CohFT calculus in the two-strand case	24
5.2.2 Khovanov ($N = 2$) case	25
5.2.3 KhR (generic N) case	26
5.2.4 Expressions for the primary polynomials as “deformed” expressions for the HOMFLY polynomials	26
5.2.5 Comparing the $N = 2$ and $N > 2$ cases	27
5.2.6 The primary polynomial as the generating function for the soliton diagrams	28
5.2.7 Example: torus knot $T^{2,5}$	29
5.3 The first-level division for particular three-strand knots	29
5.3.1 A draft of the three-strand reduction procedure	29
5.3.2 Explicit formulas for the three-strand (deformed) \mathcal{R} -matrices	31
5.4 The generating function for the three-strand soliton diagrams	32
5.4.1 Guide to the experimental data	32
6 Further directions	33
A Basic properties of the special point operators	36
A.1 Constraints on the \mathcal{R} -matrices	36
A.2 Relations between the \mathcal{R} and \mathcal{Q} -matrices	36
A.3 Properties of the particular solution	38
B The “graded” basis respected by the differentials	38
C Morphisms of the representation spaces. A more involved example	39
D List of braids providing the unique level I reminders	40
E Examples of the unique minimal remainders related to the CohFT diagrams in the case of three strands	41
E.1 The doubly twisted diagram of the unknot	41
E.2 The trefoil knot in different three strand presentations	42
E.3 The “thick” knot 8_{19} (torus $T[3, 4]$)	47

1 Introduction

Proposed less than 20 and a little more than 10 years ago, the Khovanov [5] and the Khovanov–Rozanski [4] (abbreviated as “KhR” throughout the text) invariants are rather young by the knot theory standards.

Table 1: Constructively defined knot invariants

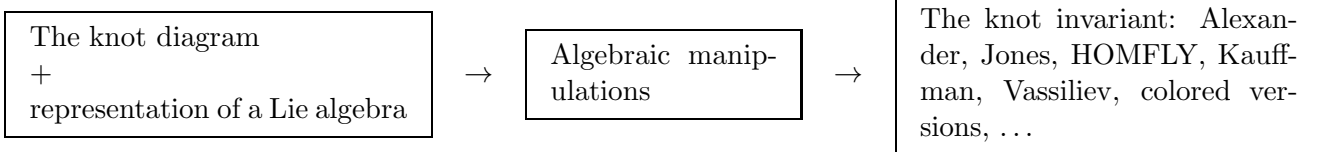
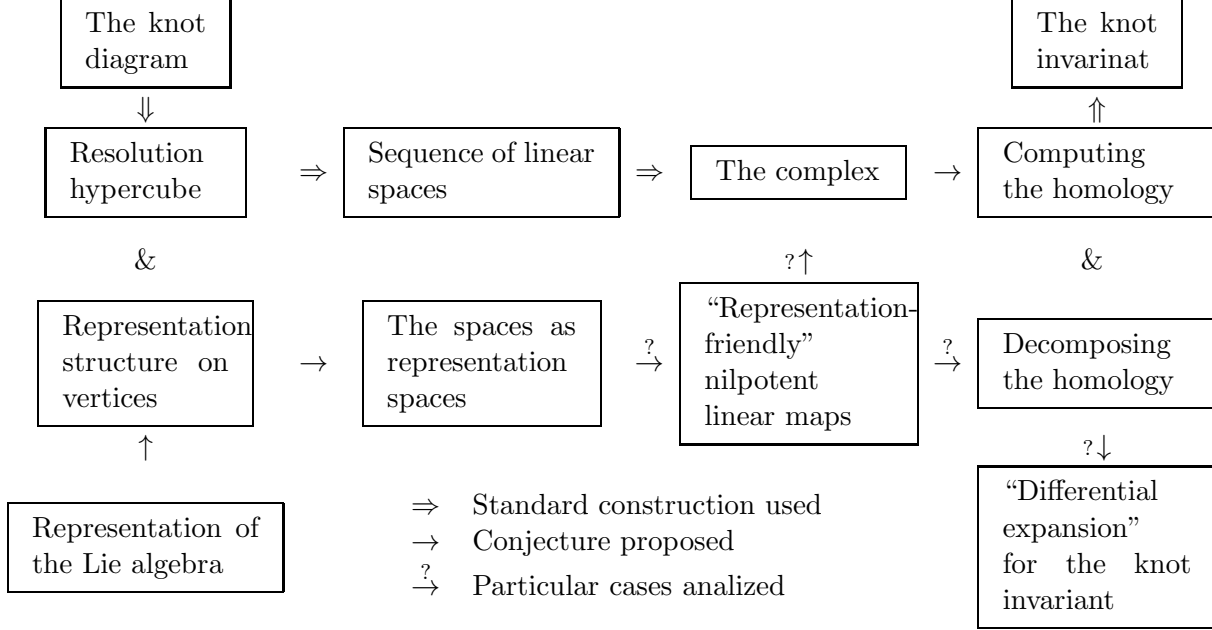


Table 2: Homological knot invariants



Relating a knot (or a link) to a function (precisely, to a polynomial) that is preserved under arbitrary continuous space transformations, the both quantities extend already wide class of the polynomial knot invariants [6, 7, 8], at the same time drastically differing from the other ones in their properties. The difference of the kind of the knot invariants is illustrated in tab. 1 and 2.

The first and the clue special point of the Khovanov, KhR and other invariants of the same kind [9] is just the definition, relating a knot to separate structure, called a *knot homology*, wherein the knot polynomial is a generating function for the basis vectors in the homologies of a certain complex (and, even worse, in the KhR case the complex itself is composed of other complexes). This sort of the definition, which is multi-level and in many points implicit, causes sever obstacles both for general analysis and for explicit computations. Searches for an alternative approach, thus being very natural, are no wonder widely expanded (see the references in tab. 3).

A closely related quantity is the *superpolynomial* of the knot [10], by now remaining among the most obscure issues of the knot theory. The superpolynomials are often studied together with the KhR invariants, the connection being two-fold. From the one hand, the superpolynomial is by its only (as far as) strict definition just an analytical continuation of the KhR polynomial (similarly to the HOMFLY invariant, which is an analytical continuation of the discrete set of the polynomials generalising the Jones polynomial¹). From the other hand, the alternative approaches developed for superpolynomials, although being neither general, nor mathematically strict in the most cases, approved themselves to be highly productive both as the research and computational tools. Hence, the interference of these two subjects may spread a light on the both quantities.

A new inspiration in the subject comes from the recently proposed *cohomological field theory* [14], (“CohFT” in our text), associated with the Khovanov and KhR invariants, like the Chern-Simons theory

¹However, the naively performed analytical continuation, well working in the HOMFLY case, runs into certain problems in the KhR case [11, 12, 3, 13], see sec. 5.2.5, 6).

was associated with the Jones and HOMFLY invariants in its time [15, 16, 17].

In the of the resent progress of various approaches to the KhR invariants, we wish to recall our own research [3], comparing it with the rigorous mathematical consideration, as well as with the alternative ways, including the newly proposed CohFT approach.

The variuos issues more or less concerned here, are summarized and enabled with the bibliographic references in table 3. The rightmost column of the table reflects the structure of the following text.

1.1 Different appoaches to KhR invariants

1.2 Conjectures and hopes

All the standpoints on the KhR invariants (or superpolynomials) different from the original one generally aim, speaking the most strictly and naively, to obtain the wanted invariants just by performing some algebraic manipulations (as many other knot invariants, including the ones mentioned in tab. 1 are obtained [6]), i.e., to pass by constructing a complex and computing homologies (at least straightforwardly).

Because the KhR formalism applies to a complex of complexes, the hope for it simplification is divided into two levels,

1. **The weak hope:** to find the explicit representation for the spaces and maps in the KhR complex.

In sec. 2 we suggest a way to do this relying on the \mathcal{R} -matrix formalism (sec. 4 contains some further details). The same way was in fact implicitly used in [3].

2. **The strong hope:** to skip computing of homologies.

This is the main idea of the minimal positive division technique, developed in [3], presented in sec. 3 in its abstract form. In 5 we attempt to combine it with the CohFT formalism from [2].

2 A sketch of the general construction

2.1 The initial set

Here we briefly review the necessary notions of the knot theory. Details can be found in any knot theory textbook, e.g., in [6].

An oriented knot in \mathbb{R}_3 . A knot \mathcal{K} is by definition an embedding of the oriented circle (e.g., a counter-clockwise direction is selected) in the three-dimensional flat space

$$\mathcal{K} : S_1 \hookrightarrow \mathbb{R}_3, \tag{2.1}$$

considered up to continuous transformations of the space \mathbb{R}_3 .

A diagram of the oriented knot. The knot can is presented by a knot diagram \mathcal{D} , which is a planar projection

$$\mathcal{D} : \mathcal{K} \rightarrow \mathbb{R}_2 \tag{2.2}$$

that minds over- and undergoings of the segments in the self-crossings (see example in fig.1). The selected direction on the knot is preserved on the knot diagram.

As a result, \mathcal{D} is planar oriented graph with four-valent vertices (self-crossings), type  or  up to continuous planar transformations.

Table 3: Summary of the discussed approaches, with bibliographic and internal references.

Khovanov polynomial			N=2
Introduced	[5]		
Computational technique developed	[18]		
Table of results, together with computer code	[7]	Presented for all prime knots (up to 11 crossings) and links (up to 11 crossings); in principle, computed for any knots	
The approach reviewed (e.g.)	[19, 20], [21, 9]		
Khovanov-Rozansky polynomial			$N \in \mathbb{Z}_+$
The definition introduced	[4]		
Applied to explicit computations	[11]	“Thin” knots up to 9 crossings	
	[22]	Knots and links up to 6 crossings, mostly for particular values of N	
The approach reviewed (e.g.)	[21, 9]		
Attempts of modification			
Tensor-like formalism	[23]	Simplest examples, 2-strand torus knots, twist knots	
\mathcal{R} -matrix bases formalism	[3]	2 and 3-strand torus knots, 3- and 4-strand knots and links up to 6 crossings, two-component links from two antiparallel strands	ssec. 2, 4
Positive division technique	[3]		ssec. 2.8, 3, 5
CoHFT approach	[14, 1, 2]		sec. 5
Superpolynomial			$0 < N_0 \leq N \in \mathbb{C}$
Introduced	[10]		
Evolution method	[24], [25], [26]		sec. 4.3
Differential expansion	[12], [25], [27], [28], [29]		sec. 4.3
Finite N problem	[11], [12], [3], [13]		ssec. 5.2.5, 6
Colored generalizations	[30], [24], [25], [27], [28], [31], [9], [32]		sec. 6

Table 4: the general plan of the construction

The resolution hypercube Σ	The complex $\mathcal{V}_0 \xrightarrow{\hat{d}_1} \mathcal{V}_1 \xrightarrow{\hat{d}_2} \dots \xrightarrow{\hat{d}_n} \mathcal{V}_n$	sec. 2.1
Vertex *	<p>A coloring (resolution) $*$ of the diagram \mathcal{D} of the knot \mathcal{K},</p> <ul style="list-style-type: none"> $n = \nu_* + \bar{\nu}_*$ 4-valent vertices, ν_*  type, $\bar{\nu}$  type ones $2m$ turning points, m either  or  type, m either  or  type ones 	sec. 2.4
	<p>The operator ${}^*\bar{\mathcal{Z}} \equiv q^{\hat{\Delta}}$ (2.7, 2.13, 2.16)</p> <p>The representation space $\mathcal{V}^* \subset V^{\circ m} = \text{Im } {}^*\bar{\mathcal{Z}}$</p>	ssec. 2.4, 2.5, 4
Edge i	The representation space V_i	sec. 2.1
A crossing, four-valent vertex $\langle k, l i, j \rangle$	An operator $V_i \otimes V_j \mapsto V_k \otimes V_l$	sec. 2
A turning point, two-valent vertex $\langle \bar{i} i \rangle$	An operator $V_{\bar{i}} \mapsto V_i$	sec. 2.4
A  vertex	The identity operator $\text{Id} \otimes \text{Id}$	sec. 2.4
A  vertex	The “double” projector $[2]_q \prod^{\wedge}$ (2.8)	sec. 2.4
An ignored turning point, $\leftarrow\sim$ or $\leftarrow\sim\sim$ type	The identity operator Id	sec. 2.4
A respected turning point, $\sim\rightarrow$ type	The operator \overrightarrow{Q} (2.7)	ssec. 2.2, 2.4
A respected turning point, $\sim\rightarrow\sim$ type	The operator \overleftarrow{Q} (2.7)	ssec. 2.2, 2.4
Directed edge $* \rightarrow *'$, $\nu_* = \nu_{*'} + 1$, $\bar{\nu}_* = \bar{\nu}_{*'} - 1$	Morphism $\mathfrak{M}_{*'}^* : \mathcal{V}^* \rightarrow \mathcal{V}^{*'} \text{, commutes with the grading operator, } \mathfrak{M}_{*'}^* \hat{\Delta} = \hat{\Delta} \mathfrak{M}_*^*$	sec. 2.6 sec. 2.5
Hyperplane $\Xi_k = \bigcup_{\bar{\nu}_* = k} *$	The representation space $\bigoplus_{\bar{\nu}_* = k} \mathcal{V}^*$	ssec. 2.6
Two subsequent hyperplanes, (Ξ_k, Ξ_{k+1})	<p>The differential $\hat{d}_k = \bigoplus_{\nu_{*'} = k+1}^{\nu_* = k} \mathfrak{M}_{*'}^*$,</p> <p>the nilpotency condition $\hat{d}_{k+1} \hat{d}_k = 0$ imposed</p>	sec. 2.6

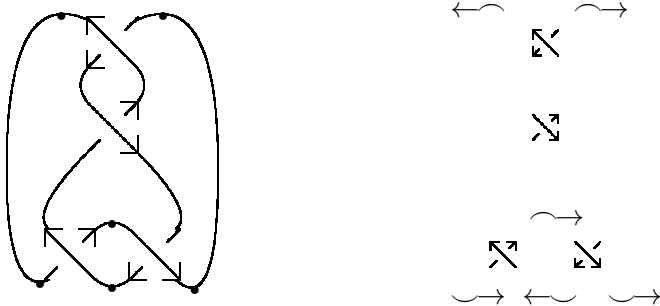


Figure 1: A diagram of the figure-eight knot and the types of the crossings and turning points.

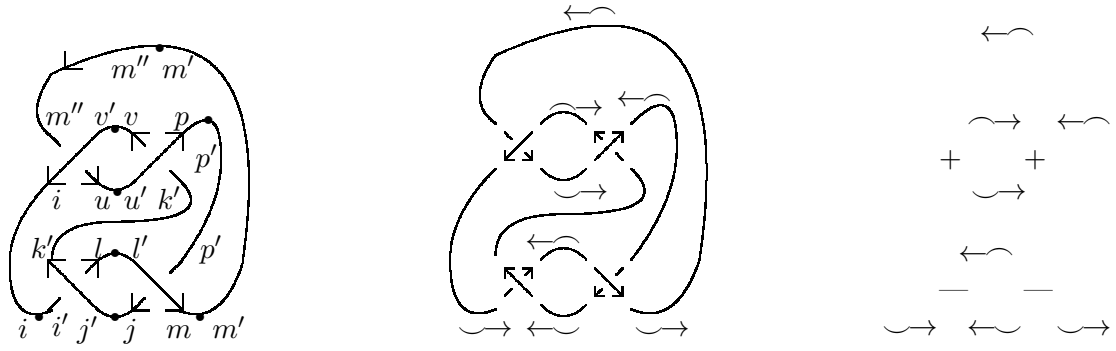


Figure 2: A diagram that represents the same knot 4_1 as fig.1 and contains only the two kinds of crossings.

The preferred direction in the projection plane. In addition, select a direction in the projection plane. Then the special points of the knot projection include, apart from the crossings, the turning points w.r.t. the direction. These points treated as the two-valent vertices on the knot diagram, type , or , or , or .

A representation space on the knot. The knot is associated with a representation space V of a Lie algebra \mathfrak{g} ,

$$\mathcal{K} \rightarrow Y \in \text{rep } \mathfrak{g} \quad (2.3)$$

i.e., one can imagine the linear space V hanged over each point of the knot. Then one can associate each edge on the knot diagram with the same space V .

Tensor presentation for knot invariants. As a result, a two-valent vertex (a turning point) of the knot diagram can be related to a linear operator $\mathcal{Q} : V \rightarrow V$, and a four-valent vertex (a crossing) can be related to a linear operator $\mathcal{R} : V \otimes V \rightarrow V \otimes V$.

The knot diagram as a diagram of the tensor contraction. The entire diagram \mathcal{D} sets then the tensor contraction of these operators. To calculate this contraction explicitly, one should

1. Enable each edge of \mathcal{D} with an integer valued label (the number of basis vector in the space V).
2. Multiply the components of \mathcal{R} and \mathcal{Q} corresponding to all the vertices.
3. Take the sum over all values of the labels (the sum sign is commonly omit in the formulas).

For some specially chosen operators \mathcal{R} and \mathcal{Q} , the tensor contraction related to the knot diagram turns out to be a topological invariant. Discussing corresponding constraints (briefly summarised in App. A) on the operators and their solutions in general is beyond the scope of our presentation. We just write down and use below all the needed explicit expressions.

2.2 The explicit expression for the knot invariants

Here we present the clue points of the \mathcal{R} -matrix approach to the knot invariants (proposed in [33, 34]; see, e.g., textbook [6], or either of papers [35, 36, 37] for a detailed review).

The tensor contraction for a knot diagram. The knot diagram must be presented so that

- The both directed segments in each self-crossing have the projections on the preferred direction of the same signs.

In particular, the self-crossings are never the turning points at the same time. One can bring a general knot diagram to the required form with help of the continuous planar transformations [6], e.g., the knot presented with the diagram in fig. 1 is presented by the diagram in fig. 2 as well.

Then, the wanted knot invariant is given by the expression

$$\mathcal{H} = \prod_{\substack{j \\ i}} \overleftarrow{\mathcal{Q}}_j^i \prod_{\substack{j \\ i \\ j}} \overleftarrow{\mathcal{Q}}_j^i \prod_{\substack{j \\ i \\ j}} \overleftarrow{\mathcal{Q}}_j^i \prod_{\substack{j \\ i \\ j}} \overleftarrow{\mathcal{Q}}_j^i \prod_{\substack{l \\ k \\ i \\ j \\ l}} \overleftarrow{\mathcal{Q}}_j^i \prod_{\substack{l \\ k \\ i \\ j \\ l}} \overleftarrow{\mathcal{R}}_{kl}^{ij} \prod_{\substack{k \\ l \\ j \\ i \\ k}} \overleftarrow{\mathcal{R}}_{kl}^{ij}. \quad (2.4)$$

E.g., for knot diagram in fig. 2 corresponds to the contraction

$$H^{(\text{fig. 2})} = \overleftarrow{\mathcal{R}}_{k'l}^{j'i'} \overleftarrow{\mathcal{R}}_{mj}^{l'p'} \overleftarrow{\mathcal{R}}_{iu}^{v'm''} \overleftarrow{\mathcal{R}}_{pv}^{u'k'} \overleftarrow{\mathcal{Q}}_{i'}^i \overleftarrow{\mathcal{Q}}_{j'}^j \overleftarrow{\mathcal{Q}}_{m'}^m \overleftarrow{\mathcal{Q}}_{l'}^l \overleftarrow{\mathcal{Q}}_u^{u'} \overleftarrow{\mathcal{Q}}_v^{v'} \overleftarrow{\mathcal{Q}}_{p'}^p \overleftarrow{\mathcal{Q}}_{m''}^{m'}. \quad (2.5)$$

The particular solution for the special point operators. Here we consider the particular series of solutions for the crossing and turning point operators. Namely, the solution for a positive integer N corresponds to the Lie group $\mathfrak{g} = su_N$, V being the space of the fundamental representation ², and (in some specially chosen basis) all the non-zero components have the explicit form³

$$\left\{ \begin{array}{lcl} \overleftarrow{\mathcal{R}}_{ii}^{ii} & = & q, \quad 1 \leq i \leq 1, \\ \overleftarrow{\mathcal{R}}_{ji}^{ij} & = & -1, \quad 1 \leq i \neq j \leq N, \\ \overleftarrow{\mathcal{R}}_{ij}^{ij} & = & q - q^{-1}, \quad 1 \leq i < j \leq N, \end{array} \right. \quad \left\{ \begin{array}{lcl} \overleftarrow{\mathcal{R}}_{ii}^{ii} & = & q^{-1}, \quad 1 \leq i \leq 1, \\ \overleftarrow{\mathcal{R}}_{ji}^{ij} & = & -1, \quad 1 \leq i \neq j \leq N, \\ \overleftarrow{\mathcal{R}}_{ij}^{ij} & = & q^{-1} - q, \quad 1 \leq i < j \leq N, \end{array} \right. \quad (2.6)$$

and

$$\overleftarrow{\mathcal{Q}}_i^i = q^{N-2i+1}, \quad \overleftarrow{\mathcal{Q}}_i^i = q^{2i-1-N}, \quad \overleftarrow{\mathcal{Q}}_i^i = 1, \quad \overleftarrow{\mathcal{Q}}_i^i = 1, \quad 1 \leq i \leq N. \quad (2.7)$$

Note that $\overleftarrow{\mathcal{Q}}_j^i = \overleftarrow{\mathcal{Q}}_j^i = \delta_j^i$, hence all the corresponding turning points can be just ignored in (2.4), just as we do from now on.

2.3 The resolution hypercube

Now we turn to the first notion both the Khovanov [5] and the KhR [4] approaches refer to, as well attempts of their modification [23, 3].

Decomposition for the crossing operators. The operators (2.6) can be identically rewritten as linear combinations of the identity operator and a projector (an operator Π^\wedge such that $\Pi^\wedge \Pi^\wedge = \Pi^\wedge$), namely,

$$\begin{aligned} \overleftarrow{\mathcal{R}} &= q \circ \mathcal{R} - \bullet \mathcal{R} = q \text{Id} \otimes \text{Id} - [2]_q \Pi^\wedge, \\ \overleftarrow{\mathcal{R}} &= q^{-1} \circ \mathcal{R} - \bullet \mathcal{R} = q^{-1} \text{Id} \otimes \text{Id} - [2]_q \Pi^\wedge. \end{aligned} \quad (2.8)$$

Formulas (2.8) are direct consequences of characteristic equations (A.8), thus being the special properties of the particular crossing operators considered here (discussed in App. A.3).

²The solution for any representation of a general Lie group is explicitly written down and discussed, e.g., in [6, 35, 38].

³We have already fixed an ambiguity in the definition of the \mathcal{Q} operators (see app. A). Note that many sources, including [6, 35] chose a different possibility.

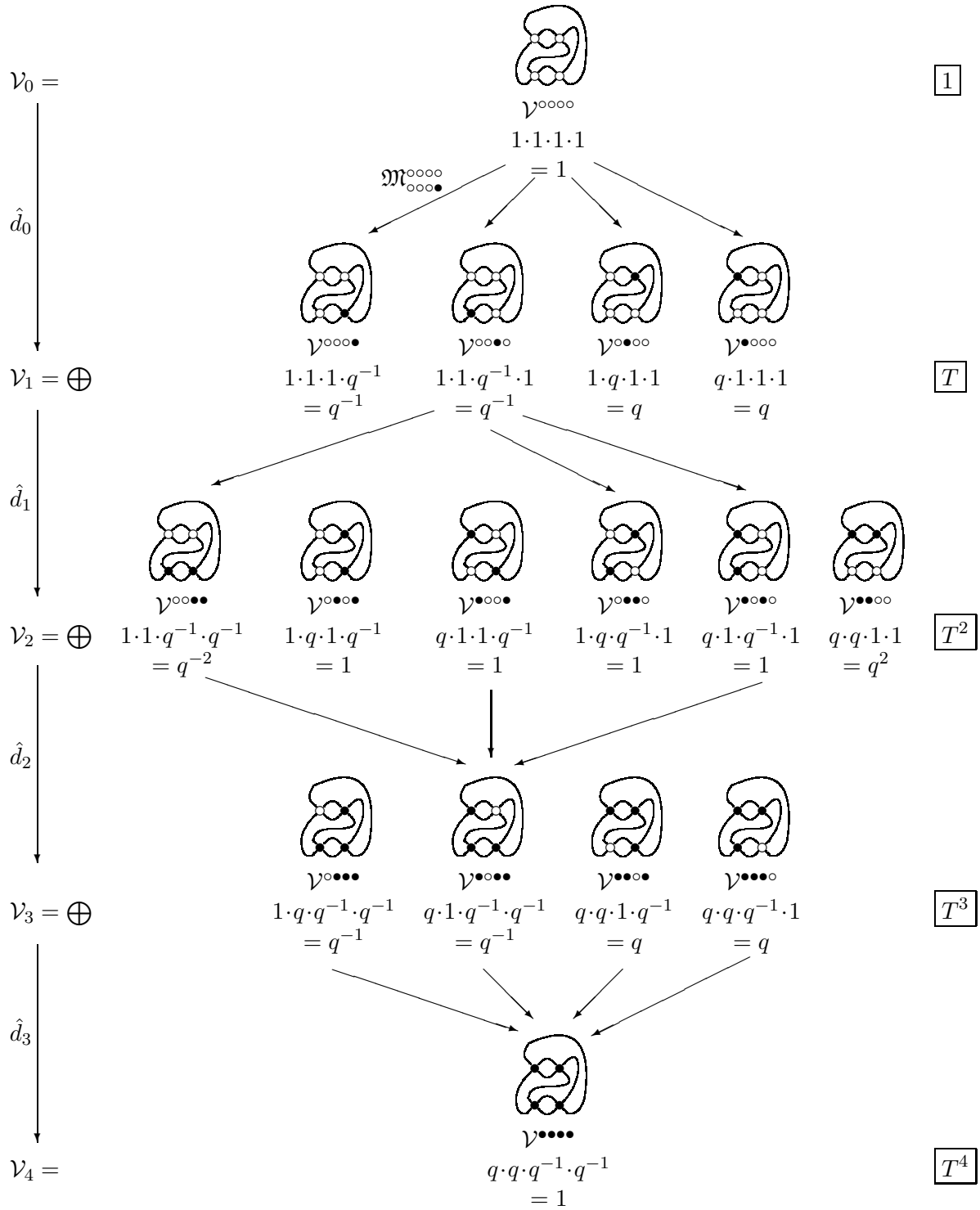


Figure 3: The resolution hypercube for the figure-eight knot (fig. 2).

A hypercube presentation for the knot invariant. The terms of the full expansion of (2.4), the crossing operators in form (2.8) substituted, can be enumerated by the various *colorings* $* \in \{\circ, \bullet\}^n$, i.e., by the partitions of the \circ and \bullet signs (associated in (2.8) with the two summands) over the n crossings.

The expansion term related to the coloring $*$ can be placed then in a vertex of the n -dimensional hypercube, a directed edge corresponding to the flip $\circ \rightarrow \bullet$ (so that a vertex $* \in \text{perm}\{\nu_* \circ, \bar{\nu}_* \bullet\}$ is connected by ν_* incoming and $\bar{\nu}_* = n - \nu$ outgoing directed edges with the overall n vertices $\{*\}' = \text{perm}\{(\nu_* + 1)\circ, (\bar{\nu}_* - 1)\bullet\}$ and $\{*\}'' = \text{perm}\{(\nu_* - 1)\circ, (\bar{\nu}_* + 1)\bullet\}$, respectively).

As a result,

- Expression (2.4) for the knot invariant is expanded over the vertices of the directed graph, called a *resolution hypercube*⁴.

For example, fig. 3 illustrates the hypercube for the diagram in fig. 2.

The generating function for the colorings. The following presentation refers to the formal series

$$\mathfrak{Z}(q, T) \equiv \mathcal{Z}(\mathcal{R}(q) \rightarrow \mathfrak{R}(q, T)) = \sum_{* \in \{\circ, \bullet\}^n} T^{\nu_*} \mathcal{Z}^*, \quad \bar{\nu}_* = \# \{\bullet \in *\}, \quad (2.9)$$

where \mathcal{Z}^* stands for the expansion term related to the coloring $*$.

Expansion (2.9) is formally obtained from expression (2.4) for the knot invariant by substituting the crossing operators with

$$\begin{aligned} \overset{+}{\mathfrak{R}}(q, T) &\equiv q \overset{\circ}{\mathcal{R}}(q) + T \overset{\bullet}{\mathcal{R}}(q) \\ \overset{-}{\mathfrak{R}}(q, T) &\equiv q^{-1} \overset{\circ}{\mathcal{R}}(q) + T \overset{\bullet}{\mathcal{R}}(q), \end{aligned} \quad (2.10)$$

or (equivalently) the matrix elements with

$$\left\{ \begin{array}{lll} \mathcal{R}_{ii}^{ii} \mapsto q, & 1 \leq i \leq 1, \\ \mathcal{R}_{ij}^{ij} \mapsto T, & 1 \leq i \neq j \leq N, \\ \mathcal{R}_{ij}^{ij} \mapsto q + q^{-1}T, & 1 \leq i < j \leq N, \\ \mathcal{R}_{ji}^{ji} \mapsto q(1 + T), & 1 \leq i < j \leq N, \end{array} \right. \quad \left\{ \begin{array}{lll} \tilde{\mathcal{R}}_{ii}^{ii} \mapsto q^{-1}, & 1 \leq i \leq 1, \\ \tilde{\mathcal{R}}_{ji}^{ij} \mapsto T, & 1 \leq i \neq j \leq N, \\ \tilde{\mathcal{R}}_{ij}^{ij} \mapsto q^{-1} + qT, & 1 \leq i < j \leq N, \\ \tilde{\mathcal{R}}_{ji}^{ji} \mapsto q^{-1}(1 + T), & 1 \leq i < j \leq N. \end{array} \right. \quad (2.11)$$

2.4 Vector spaces at the hypercube vertices

The next step inputs the representation theory data in the construction (see, e.g., [38] for needed background). The following presentation is equivalent to the standard presentation of the Khovanov construction [5] in the particular case of the su_2 algebra (details can be found in [6]), and it is very plausible to reproduce the KhR construction [4] in the more general case of su_N , although in somewhat different notions⁵.

The operators related to a coloring. The $\overset{+}{\mathfrak{Z}}$ contribution to (2.4), related to the coloring $*$ (ν_* items of \circ , $\bar{\nu}_*$ items of \bullet , $n = \nu_* + \bar{\nu}_*$ overall), identically equals to the contraction of the operators (we omit the operators $\overset{\leftarrow}{\mathcal{Q}}_j^i = \overset{\leftarrow}{\mathcal{Q}}_j^i = \delta_j^i$)

$$\mathcal{Q}^{\circ m} \Big|_J^I = \prod_{\substack{i \\ \circ}} \overset{\leftarrow}{\mathcal{Q}}_j^i \prod_{\substack{i \\ \bullet}} \overset{\leftarrow}{\mathcal{Q}}_j^i \quad (2.12)$$

⁴In a graphical presentation for the tensor contractions, the expansion terms are associated with the various *resolutions* of the knot diagram.

⁵First, the two resolutions of a crossing in [4] are related to the same two addends in decomposition (2.8) for the su_N \mathcal{R} -matrix in the fundamental representation [38]. Second, the spaces in the Resolution hypercube vertices (and further of the spaces in the resulting complex), are described in [4] as the complexes of commutative polynomial rings, which at the same time are for description of the su_N representation spaces in terms of the BGG resolvents [39] (the author is indebted to I.Danilenko for pointing out to this observation and giving the reference).

(m being the number of the “left-to-right” turning points ⁶, which we only account for) and

$${}^*\mathcal{Z}_J^I \equiv q^{\nu_+ - \nu_-} \prod_{l \in \text{outgoing}} {}^{\circ}\mathcal{R}_{kl}^{ij} \prod_{l \in \text{ingoing}} {}^{\bullet}\mathcal{R}_{kl}^{ij}, \quad * \in \{\circ, \bullet\}^n, \quad (2.13)$$

where the q power the form factor explicitly depends on the numbers ν_+ and ν_- of, respectively, the  and  type crossings substituted with ,

$$\nu_+ = \#\left\{ \text{crossing with a dot on the top-left edge} \rightarrow \text{crossing with a dot on the top-left edge} \in \mathcal{D}^* \right\}, \quad \nu_- = \#\left\{ \text{crossing with a dot on the bottom-left edge} \rightarrow \text{crossing with a dot on the bottom-left edge} \in \mathcal{D}^* \right\}. \quad (2.14)$$

(This factor appears as a charge for expressing the both ${}^+\mathcal{R}$ and ${}^-\mathcal{R}$ through the same pair  and ). The multi-indices I and J are defined as the sets of the labels attached to all the edges incoming and outgoing the turning points, respectively, i.e.,

$$I = \left\{ \bigcup_{i \in \text{ingoing}} \bigcup_{j \in \text{outgoing}} i \right\}, \quad J = \left\{ \bigcup_{i \in \text{outgoing}} \bigcup_{j \in \text{ingoing}} j \right\}. \quad (2.15)$$

Hence, both operators $\mathcal{Q}^{\circ m}$ and ${}^*\mathcal{Z}$ are defined on the tensor power $V^{\circ m}$ of the original space V , m being the number of the non-unity turning points in the knot diagram. In the following we also consider the composition of these operators

$${}^*\bar{\mathcal{Z}} \equiv \mathcal{Q}\mathcal{Z}. \quad (2.16)$$

Contraction (2.4) can be then equivalently presented as the trace

$$\mathcal{H} = \text{Tr}_{V^{\circ m}} \mathcal{Q}\mathcal{Z} = \text{Tr}_{V^{\circ m}} \mathcal{Q}^{\circ m} \mathcal{Z} = \text{Tr}_{V^{\circ m}} {}^*\bar{\mathcal{Z}}. \quad (2.17)$$

2.5 Spaces at vertices as graded spaces

The Khovanov [5] and the KhR [4] constructions both essentially use one more notion, in fact related to representation theory of quantum groups [38]. Namely, a special (*graded*) basis is considered in each vertex of the hypercube. Below we give the \mathcal{R} -matrix description of these spaces, in fact used for explicit computations in [3].

Spaces at vertices as image spaces One can also show that⁷

$${}^*\bar{\mathcal{Z}}({}^*\bar{\mathcal{Z}}(\mathcal{V})) = {}^*\bar{\mathcal{Z}}(\mathcal{V}) \subset V^{\mathcal{D}}, \quad (2.18)$$

i.e., the operator , originally defined on the space $V^{\circ m}$, can be treated as an isomorphism of its image space, i.e.,

$$\boxed{{}^*\bar{\mathcal{Z}} : \mathcal{V}^* \equiv \text{Im} {}^*\bar{\mathcal{Z}} \Big|_{V^{\circ m}} \rightarrow \mathcal{V}^*}, \quad (2.19)$$

In all the following, we

⁶Then the diagram has $2m$ turning points overall. Indeed, the numbers of turning points of various kinds on a closed curve satisfy $\begin{cases} \# \{\leftarrow \curvearrowright\} + \# \{\curvearrowleft \rightarrow\} = \# \{\leftarrow \curvearrowright\} + \# \{\curvearrowleft \rightarrow\} \\ \# \{\leftarrow \curvearrowright\} + \# \{\leftarrow \curvearrowleft\} = \# \{\curvearrowright \rightarrow\} + \# \{\curvearrowleft \rightarrow\} \end{cases}$, and the termwise subtracting of these equations (two ways) yields $\# \leftarrow \curvearrowright = \# \curvearrowleft \rightarrow$ and $\# \leftarrow \curvearrowleft + \# \curvearrowright \rightarrow$.

⁷The operators \mathcal{R} ($* \in \{\circ, \bullet\}$) defined in (2.8), satisfy $\mathcal{R}^2 \sim {}^*\mathcal{R}$, so that, if $y \in \text{Im} {}^*\mathcal{R}$, then $y = {}^*\mathcal{R}^2 x = {}^*\mathcal{R} x \in {}^*\mathcal{R}(V)$ and hence the same is true for , which by definition (2.13) is a tensor product of the operators . The same is true for the operator , because $\mathcal{Q}\mathcal{Z} = {}^*\mathcal{Z}\mathcal{Q}$ for any  (due to the “built in” representation theory properties of these operators [38]) so that $x = \mathcal{Q}\mathcal{Z}({}^*\mathcal{Z}y) = \mathcal{Q}^2 {}^*\mathcal{Z}^2 y \Rightarrow x = \mathcal{Q}^2 {}^*\mathcal{Z}z = \mathcal{Q}\mathcal{Z}(\mathcal{Q}y)$, i.e.,  $\equiv \mathcal{Q}\mathcal{Z}(\mathcal{V}) \subset {}^*\bar{\mathcal{Z}}^{-1}\mathcal{V} \subset \mathcal{V} \Rightarrow \mathcal{V} \subset {}^*\bar{\mathcal{Z}}\mathcal{V}$ (above relations imply that the operator is invertible). Hence,  $= \mathcal{V}$, as claimed.

- Relate a coloring $*$ to the space \mathcal{V}^* defined by (2.19), with ${}^*\bar{\mathcal{Z}}$ defined in (2.13, 2.16) and “place” this space in the corresponding hypercube vertex.

Basis of eigenvectors as a graded basis. Moreover, the operator ${}^*\bar{\mathcal{Z}}$ has a basis of the eigenvectors the subspace \mathcal{V}^* , the eigenvalues being q powers,⁸

$$\left\{ \mathcal{X}_\alpha^* : {}^*\bar{\mathcal{Z}}\mathcal{X}_\alpha^* = q^{\Delta_\alpha} \mathcal{X}_\alpha^* \right\}_{I=1}^{\dim \mathcal{V}^*}. \quad (2.20)$$

Hence, one can consider the linear space

$$v^* \equiv \text{span} \{ q^{\Delta_\alpha} \}, \quad (2.21)$$

with the contraction

$$\mathfrak{P}^*(q) \equiv \text{Tr } v^* {}^*\bar{\mathcal{Z}} \quad (2.22)$$

as a generating function for the monomial basis. The introduced in [3] as the *primary polynomial* coincides then with the two-variable generating function,

$$\mathfrak{P}(q, T) \equiv \mathcal{H}(\mathcal{R} \rightarrow \mathfrak{R}) = \sum_* T^{\nu_*} \mathfrak{P}^*(q). \quad (2.23)$$

- Relations (2.22, 2.23) associates each term in the primary polynomial with a vector of the linear space placed at one of the resolution hypercube vertices.

2.6 From the resolution hypercube to the complex

The last step of the Khovanov [5]/KhR [4] constructions consists in relating the Resolution hypercube directed edges to the certain maps (the *morphisms*). These maps must respect the graded bases earlier related to the hypercube vertices, and this severely constraints the form of the morphisms.⁹

The resolution hypercube is then transformed into the Khovanov/KhR complex in a canonic way [5, 4].

Maps associated with edges as maps of the graded spaces. An edge of the hypercube is by definition directed from a coloring $*$ to a coloring $*'$ obtained by the change $\circ \rightarrow \bullet$ in only one vertex. The edge corresponds to a *morphism*, i.e., to a linear map

$$\mathfrak{M}_{*'}^* : \mathcal{V}^* \rightarrow \mathcal{V}^{*'} . \quad (2.24)$$

Here we do not determine this map explicitly¹⁰, but formulate an essential constraint we highly rely on in all the following¹¹. Namely,

- The maps acting along the edges must commute with the maps ${}^*\bar{\mathcal{Z}}$ of the spaces of the hypercube vertices,

$\mathfrak{M}_{*'}^* {}^*\bar{\mathcal{Z}} = {}^*\bar{\mathcal{Z}} \mathfrak{M}_{*'}^* .$

(2.25)

Relation (2.25) implies that an eigenvector $\mathcal{X} \in \mathcal{V}^*$ of ${}^*\bar{\mathcal{Z}}$, is mapped to an eigenvector $\mathcal{X}' \in \mathcal{V}^{*'}$ of ${}^{*'}\bar{\mathcal{Z}}$ with the same eigenvalue,

$${}^*\bar{\mathcal{Z}}\mathcal{X} = q^\Delta \mathcal{X} \Rightarrow {}^{*'}\bar{\mathcal{Z}}\mathcal{X}' = {}^{*'}\bar{\mathcal{Z}}\mathfrak{M}_{*'}^*\mathcal{X} = \mathfrak{M}_{*'}^* {}^*\bar{\mathcal{Z}}\mathcal{X} = q^\Delta \mathfrak{M}_{*'}^*\mathcal{X} = q^\Delta \mathcal{X}' . \quad (2.26)$$

The same statement in terms of the introduced above gradings reads

⁸Same to the previous property, these facts follows from definitions (2.13, 2.16), form the commutation relation $\mathcal{Q}{}^*\bar{\mathcal{Z}} = {}^*\bar{\mathcal{Z}}\mathcal{Q}$, and from the corresponding facts being valid for the \mathcal{R} ($* \in \{\circ, \bullet\}$).

⁹The morphisms are described in [4] as ring homomorphisms.

¹⁰See [4] for the original definition, [22, 11] for adoptations to the explicit computations, and [23] for an attempt to give an alternative definition.

¹¹Some further properties of the maps are discussed in sec. 4

- Morphism (2.24) maps a graded vector $\mathcal{X} \in \mathcal{V}^*$ to the graded vector $\mathcal{X}' \in \mathcal{V}'^*$ with the same grading¹².

The grading respecting differentials. To obtain the complex, one should first construct a sequence of linear spaces that are direct sum of the spaces at separate hypercube vertices. Namely, the sum for the space k includes all colorings with $\nu_* = k$ items of \bullet ,

$$\mathcal{V}_k = \bigoplus_{\nu_* = k} \mathcal{V}^*, \quad k = \overline{0, n}. \quad (2.27)$$

The differential \hat{d}_k maps then space $k-1$ to space k as a direct algebraic sum of the corresponding morphisms,

$$\bigoplus_{\nu_{*'} = k+1}^{\nu_* = k} (-1)^{\text{par}* + \text{par}*' \mathfrak{M}_{*'}^*} \mathfrak{M}_{*'}^* \equiv \hat{d}_k : \mathcal{V}_k \rightarrow \mathcal{V}_{k+1}, \quad k = \overline{0, n-1}, \quad (2.28)$$

where the $\text{par}* = 0, 1$ stands for the parity of the corresponding coloring (the two colorings have the opposite parities, whenever differing by the only permutation $\boxtimes \leftrightarrow \boxtimes$; see, either of the cited papers (e.g. [5]) for the precise definition).

The differentials defined by (2.28) are by construction nilpotent (subsequently orthogonal),

$$\hat{d}_k \hat{d}_{k-1} = 0, \quad k = \overline{1, n}, \quad (2.29)$$

and commute with the coloring operators ${}^* \bar{\mathcal{Z}}$ (because all the morphisms do),

$$\mathcal{Z}_{k+1} \hat{d}_k = \hat{d}_{k+1} \mathcal{Z}_k \quad \text{with} \quad \mathcal{Z}_k \equiv \bigoplus_{\nu_* = k} \mathcal{V}^*. \quad (2.30)$$

In other words,

- Starting from the resolution hypercube, the linear spaces at the vertices, the morphisms along the directed edges, one constructs a sequence of the space associated with entire hyperplanes and sequence of the nilpotent grading-preserving¹³ linear maps, the *differentials*. The obtained sequences compose the wanted *complex*.

2.7 Graded basis in the homologies

In fact, a graded bases in each space is so far selected up to arbitrary changes involving the spaces with the same gradings. Below we describe a more special basis, which is the union of the graded bases in the image, co-image and the homology subspaces of the differentials in the complex. A more detailed derivation is given in B.

Nilpotency condition (3.2) implies that

$$x \in \text{Im } \hat{d}_k \subset V_k \stackrel{\text{def}}{\Leftrightarrow} x = \hat{d}_k y \Rightarrow x \in \ker \hat{d}_{k+1} \subset V_{k+1} \stackrel{\text{def}}{\Leftrightarrow} \hat{d}_{k+1} x = 0 \quad (2.31)$$

The inverse is generally wrong. The homology space is by definition the *factor space*¹⁴

$$H_k \stackrel{\text{def}}{=} \ker \hat{d}_{k+1} / \hat{d}_k \subset V_{k+1}, \quad \text{i.e.,} \quad x \in H_k \Leftrightarrow \hat{d}_k x = 0 \ \& \ \hat{d}_k y \neq x, \quad \forall y \in V_k \quad (2.32)$$

Just from the definitions (in particular, $x \in \text{coIm } \hat{d} \stackrel{\text{def}}{\Leftrightarrow} \hat{d}x \neq 0$),

$$\mathcal{V}_k = \text{Im } \hat{d}_k \oplus \text{coIm } \hat{d}_{k+1} \oplus H_k. \quad (2.33)$$

A non-trivial consequence of property (2.30) of the considered differentials is that

¹²In fact, only that a graded vector is mapped to a graded vector is essential, while the equality of the gradings ($\Delta = \Delta'$) is related to a freedom in the definition of the morphisms (i.e., there are different possibilities that ultimately yield the same knot invariant). A more conventional choice (in particular, used in [5, 18, 4, 22, 19, 20, 23, 32]) provides the grading lowered by the morphisms so that $\Delta' = \Delta - 1$.

¹³See the above footnote in the definition of the morphisms.

¹⁴Rigorously speaking, a vector of the homology subspace $x \in H_k$ is defined up to an arbitrary vector from the Image subspace, $x \sim x + \hat{d}_k y, \forall y \in V_k$.

- Each of the three spaces in decomposition (2.33) contains a graded basis.

Precisely, a basis in the space \mathcal{V}_k can be composed of the three groups of the vectors (see App. B),

$$\left\{ y_{k,i} : \hat{d}_{k+1} y_{k,i} \neq 0 \right\}_{i=1}^{\dim \text{Im } \hat{d}_{k+1}} \cup \left\{ z_{k,i} = \hat{d}_k y_{k-1,i} \right\}_{i=1}^{\dim \text{Im } \hat{d}_k} \cup \left\{ h_{k,i} \right\}_{i=1}^{\dim \mathcal{V}_k - \dim \text{Im } \hat{d}_k - \dim \text{Im } \hat{d}_{k+1}}, \quad (2.34)$$

$$\hat{\Delta} y_{k,i} = \Delta_{k,i} y_{k,i} \quad \hat{\Delta} z_{k,i} = \Delta_{k-1,i} z_{k,i} \quad \hat{\Delta} h_{k,i} = \Delta'_{i,k} h_{i,k}.$$

2.8 The geometric sense of the positive integer" decomposition

Here we address to the finite issue of this section content, namely to derivation of the positive integer decomposition for the primary polynomial from [3] in the discussed notions.

Calculating trace (2.17) in basis (2.34) yields the following decomposition for the generating function

$$\begin{aligned} \mathfrak{P}(q, T) = \sum_{k=0}^n T^k \text{Tr } \mathcal{V}_k q^{\hat{\Delta}} &\equiv \sum_{k=0}^n T^k \dim_q \mathcal{V} = \sum_{k=0}^n T^k \left(\text{Tr}_{\text{colIm } \hat{d}_{k+1}} q^{\hat{\Delta}} + \text{Tr}_{\text{Im } \hat{d}_k} q^{\hat{\Delta}} + \text{Tr}_{H_k} q^{\hat{\Delta}} \right) \stackrel{(2.34)}{=} \\ &= \sum_{k=0}^n T^k \left(\sum_{i=1}^{\dim \text{Im } \hat{d}_{k+1}} q^{\Delta_{k,i}} + \sum_{i=1}^{\dim \text{Im } \hat{d}_k} q^{\Delta_{k-1,i}} + \sum_{i=1}^{\dim H_k} q^{\Delta'_{k,i}} \right) = \\ &= \sum_{k=0}^{n-1} \left(T^k + T^{k+1} \right) \sum_{i=1}^{\dim \text{Im } \hat{d}_{k+1}} q^{\Delta_{k,i}} + \sum_{k=0}^n T^k \sum_{i=1}^{\dim H_k} q^{\Delta'_{k,i}} = (1+T) \mathcal{J}(q, T) + \mathcal{P}(q, T). \quad (2.35) \end{aligned}$$

Note that the coefficient of each power $q^{\hat{\Delta}}$, both in $\mathcal{J}(q, T)$ and $\mathcal{P}(q, T)$, as well as in $\mathfrak{P}(q, T)$, is nothing but the multiplicity of the basis vector from the corresponding subspace ($\oplus_{k=1}^n \text{Im } \hat{d}_k$, $\oplus_{k=0}^n H_k$ or $\oplus_{k=0}^n \mathcal{V}_k$, respectively) with the grading Δ . This leads to the essential property of the obtained decomposition,

- All three quantities in decomposition (2.35), the divident $\mathfrak{P}(q, T)$, the quotient $\mathcal{J}(q, T)$ and the remainder $\mathcal{P}(q, T)$ are sums of the q and T powers with *positive integer* coefficients.

3 A minimal positive division instead of computing the homology

In this section, we wish to discuss the idea of the positive integer" division as a shortcut in homology computing in very general terms, separately from the knot theory applications.

Through the section, the spaces V , the maps \hat{d} and all the related quantities are not associated any how with the particular complexes arising the knot theory. Beside that, here we consider plain, not graded linear spaces, because a graded complex (see sec. 2.5) is always a direct sum of ordinary complexes. As well, we do not consider any additional structures on the linear spaces, like Lie algebra \mathfrak{g} (this is the case of the next section, sec. 4).

3.1 General definitions

3.1.1 Complex, homologies and decomposition of the generating functions.

Denied that the most needed definitions and theorems are already given above in sec. 2, we present them below in a compressed form for convenience.

Generally, a complex [40] is a defined as a sequence of linear spaces and linear maps of each space to the subsequent one,

$$0 \xrightarrow{\hat{d}_0} V_0 \xrightarrow{\hat{d}_1} V_1 \xrightarrow{\hat{d}_2} V_2 \xrightarrow{\hat{d}_3} \dots \xrightarrow{\hat{d}_n} V_n \xrightarrow{\hat{d}_{n+1}} 0, \quad (3.1)$$

such that any pair of the subsequent maps satisfy the *nilpotency* condition.

$$\hat{d}_2 \hat{d}_1 = \hat{d}_3 \hat{d}_2 = \dots = \hat{d}_n \hat{d}_{n-1} = 0. \quad (3.2)$$

Condition (3.2) in particular implies that $\text{Im } \hat{d}_k \subset \ker \hat{d}_{k+1}$ ($k = \overline{0, n}$), and the homology in term k is the *factor space*

$$H_k \equiv \ker \hat{d}_{k+1} / \text{Im } \hat{d}_k, \quad (3.3)$$

i.e., a subspace of kernel vectors any two differing by an image vector is by definition treated as the single homology element,

$$\begin{aligned} x \in H_k &\Rightarrow \hat{d}_{k+1}x = 0, \\ x \sim y \in H_k &\Leftarrow \hat{x} - y = \hat{d}_k z \quad \left(\stackrel{(3.2)}{\Rightarrow} \hat{d}_{k+1}x = \hat{d}_{k+1}y = 0 \right). \end{aligned} \quad (3.4)$$

The generating functions in formal variable T

$$\mathcal{F} \equiv \sum_{k=0}^n T^k \dim V_k, \quad \mathcal{J}(T) \equiv \sum_{k=0}^n T^k \dim \text{Im } \hat{d}_k, \quad \mathcal{P} \equiv \sum_{k=0}^n T^k \dim H_k \quad (3.5)$$

for the dimensions of the linear spaces, the image subspaces and the homologies ¹⁵ satisfy the relation (a particular case of (2.35), when $q = 1$ so that $\dim_q \rightarrow \dim$)

$$\boxed{\mathcal{F}(T) = \mathcal{P}(T) + \mathcal{J}(T)(1 + T).} \quad (3.6)$$

In the following, we call (3.6) a *positive integer decomposition* for the generating function, because

- All the coefficients of the T powers in $\mathcal{F}(T)$, $\mathcal{P}(T)$ and $\mathcal{J}(T)$ are by definitions the positive integer numbers (the dimensions of the corresponding subspaces).

We study the question,

- To what extend one can recover the remainder $\mathcal{P}(T)$ from the divident $\mathcal{F}(T)$ **avoiding** the straightforward computing the homology?

The realization of the Strong hope formulated in the introduction is associated with the progress on this way.

Treated as an isolated algebraic problem, the above question can possess no satisfactory answer, not being even formulated rigorously. Below we attempt specify a problem to study, applying to various additional considerations based on the known properties of the knot homologies [3].

3.1.2 Integer and polynomial division.

The polynomial division is a straightforward extension of the integer division¹⁶. The the both kinds of the problem is formulated in the table below (the given quantities are underlined, the quantities to find are marked by the question sign).

Integer division			Polynomial division (variable T)		
$m, k, q, p \in \mathbb{Z}$			$\mathcal{F}(T), \mathcal{G}(T), \mathcal{J}(T), \mathcal{P}(T) \in \text{Pol}(T)$		
<u>divident</u>	<u>divider</u>	<u>quotient</u>	<u>divident</u>	<u>divider</u>	<u>quotient</u>
m	k	q	$\mathcal{F}(T)$	$\mathcal{G}(T)$	$\mathcal{J}(T)$
					$\mathcal{P}(T)$
					?
					?
ambiguity		constraint	ambiguity		
$k \rightarrow q + u, p \rightarrow p - ku, u \in \mathbb{Z}$	$0 \leq p < q$	$\mathcal{J} \rightarrow \mathcal{J} + f(T), \mathcal{P} \rightarrow \mathcal{P} - f(T)Q, f(T) \in \text{Pol}(\mathbb{Z} T)$			

¹⁵The function $\mathcal{P}(T)$ is referred to as the *Poincare polynomial* of the complex; in particular, $\chi \equiv \mathcal{P}(T = -1)$ is the *Euler character* of the complex.

¹⁶It is the multivariable division in fact applied to the KhR calculus, but we do not discuss the difference here.

In the both cases the equality in row 3 does not define the unknown uniquely. Namely, the equality still holds, as the both the quotient and the remainder are subjected to the transformation in the last row. In the integer case, the ambiguity is conventionally fixed by the constraint given in the same line. The polynomial case is essentially different in this point. Namely, non of the formal ways to select the unique remainder (now defined up to a polynomial instead of just an integer) *a priori* produces a quantity adequate for a certain application.

3.1.3 Division as computing homology

Now we give an elementary illustration to the main idea we use, namely to the correspondence between the homology calculus and the polynomial division, with a freedom in definition of the remainder (see the last line in tab. 3.7 and the comment in the end of sec. 3.1.2). Below we take a simple particular case of division problem with, and construct two different complexes, the homologies producing two different remainders.

In the context of the knot polynomials, we in fact deal with the very special case of the right column of tab. 3.7, when all the polynomials have all positive integer coefficients, and the divider is the binomial $(1 + T)$. The general problem we consider is to present a given polynomial $\mathcal{F}(T)$ in the form

$$\boxed{\mathcal{F}(T) = (1 + T)\mathcal{J}(T) + \mathcal{P}(T)} \quad (3.8)$$

$$\mathcal{F}(T) = \sum_{k=0}^n a_k T^k, \quad \mathcal{J}(T) = \sum_{k=0}^m b_k T^k, \quad \mathcal{P}(T) = \sum_{k=0}^l c_k T^k, \quad \{a_k, b_k, c_k\} \subset \mathbb{Z}_+.$$

(A large freedom in the definition of the remainder yet presents even in this particular case, as we will see in the examples below.)

In the described particular case the division problem is straightforwardly related to a homology computing problem. Namely, extracting the $\sim (1 + T)$ part is equivalent to matching the monomial addends in the pairs (x, Tx) , each monomial entering just one pair, some monomials remain unpaired in a general case. E.g., $\mathcal{F}(T) = 3 + 4T + T^2$ admits the two matchings, each with one unpaired monomial,

$$\begin{array}{c} \underline{3 + 4T + 2T^2} = \\ \begin{array}{c|c} \begin{array}{c} 3 + 3T \\ + T + T^2 \\ \bullet \longrightarrow \bullet + \boxed{T^2} \\ \bullet \longrightarrow \bullet \\ \bullet \longrightarrow \bullet \hat{d}_1 \\ \hat{d}_0 \bullet \longrightarrow \bullet \\ \bullet \end{array} & \begin{array}{c} 1 + \\ 2 + 2T \\ \bullet + 2T + 2T^2 \\ \bullet \longrightarrow \bullet \\ \bullet \longrightarrow \bullet \hat{d}_1 \\ \hat{d}_0 \bullet \longrightarrow \bullet \\ \bullet \end{array} \end{array} \\ \hline (1 + T) \cdot (3 + T) + \boxed{T^2} & \boxed{1} + (2 + 2T) \cdot (1 + T) \end{array} \quad (3.9)$$

In either diagram in (3.9), a bullet is placed in column $k+1$ for each the T^k addend in \mathcal{F} of the corresponding diagram, the arrows label the matching pairs. The positions of arrows matching column k with column $k+1$ can be then represented by the matrix \hat{d}_{k-1} such that $d_{k-1}^{ij} = 1$ if bullet i in column k matches bullet j in column $k+1$, and $d_{k-1}^{ij} = 0$ otherwise. Then, the two particular diagrams in (3.9) give rise to the matrices

$$\hat{d}_1 = \begin{pmatrix} 0 & 0 & 0 & 0 \end{pmatrix}, \quad \hat{d}_0 = \begin{pmatrix} 1 & 0 & 0 \\ 0 & 1 & 0 \\ 0 & 0 & 1 \\ 0 & 0 & 0 \end{pmatrix}, \quad \text{and} \quad \hat{d}_1 = \begin{pmatrix} 1 & 0 & 0 & 0 \\ 0 & 0 & 0 & 1 \end{pmatrix}, \quad \hat{d}_0 = \begin{pmatrix} 0 & 0 & 0 \\ 0 & 1 & 0 \\ 0 & 0 & 1 \\ 0 & 0 & 0 \end{pmatrix}. \quad (3.10)$$

In the both cases $\hat{d}_1 \hat{d}_0$, due to each bullet entering no more than one pair. Hence, if a column is associated with a linear space (a bullet for a basis vector), the arrows set the differentials with the matrices (3.10). One thus obtains the complex, the homology spanned over the basis vector corresponding to the unpaired bullet (related to the remainder in the division problem).

3.2 “Ambigiuos” and “anambigiuos” minimal remainders

As already discussed in sec. 3.1.2, decomposition (3.8) is not unique. The first and the most naive constraint we impose on the remainder is

- The remainder $\mathcal{P}(T)$ contains the miminal possible number of different T powers.

Although this requirement defines the unique remainder only in particular cases, it turns out to be very useful in application to the knot polynomials (see [3] and sec. 5). Moreover, all further, more involved constraints we treat refer to the this, elementary one.

Here we consider in details the simplest examples, when the $\mathcal{F}(T)$ contains up to three subsequent T powers¹⁷. The “minimal” (in the specified sense) remainders of the minimal positive division, together with remaining ambiguity (if presents) are given for the various relations between the coefficients in the divident in tables¹⁸ (3.11–3.12). As one can see from table (3.12), already the case of the three-term divident appears to be rather non-trivial.

$\mathcal{F}(T) = aT^k$	
Type	Unambigous
$\mathcal{J}(T)$	0
$\mathcal{P}(T)$	$a_0 T^k$

$\mathcal{F}(T) = a_0 + a_1 T, \quad \chi \equiv a_0 - a_1$			
Type	Unambigous		
Case	$\chi > 0$	$\chi = 0$	$\chi < 0$
$\mathcal{J}(T)$	$\chi + a_1(1 + T)$	$a_0(1 + T)$	$(-\chi)T + a_0(1 + T)$
$\mathcal{P}(T)$	a_1	$a_0 = a_1$	a_0
	χ	0	$(-\chi)T$

$\mathcal{F}(T) = a_0 + a_1 T + a_2 T^2, \quad \chi \equiv a_0 - a_1 + a_2$					
Type	Unambigous			Ambigous	
Case	$\chi \leq 0$		$\chi > 0$		
	$a_0 \leq a_1 < a_2$	$a_2 \leq a_1 < a_0$	$a_1 < a_0, a_1 < a_2$	$a_0 \leq a_1, a_2 \leq a_1$	
$\mathcal{J}(T)$	$a_0 + a_2 T$	$a_0 + (a_1 - a_0)T$	$(a_1 - a_2) + a_2 T$	$(a_0 - p) + (p - a_0 + a_1)T$	$(a_1 - a_2) + a_2 T;$ $a_0 + (a_1 - a_0)T$
$\mathcal{P}(T)$	$(-\chi)T$	χT^2	χ	$p + (\chi - p)T^2$	$\chi;$ χT^2
E.g.	$1 + 3T + T^2$	$1 + T + 2T^2$	$2 + T + T^2$	$3 + 2T + 4T^2 =$	$3 + 4T + 2T^2 =$
	$= T +$ $(1 + T)^2$	$= T^2 +$ $(1 + T)^2$	$= 1 +$ $(1 + T)^2$	$(1 + 4T^2) + 2(1 + T)$ $= (2 + 3T^2) + (1 + T)^2$	$T^2 + (1 + T)(1 + 2T)$ $= 1 + 2(1 + T)^2$

3.3 Properties of maps as “selection rules” for the “minimal remainder”

In this section we recall the homology computing problem (formulated in sec. 3.1.1) underlying the considered minimal positive division problem (formulated in sec. 3.1.2). Below we explore, in the simplest cases, how the particular known properties of the differentials may help to determine the “minimal remainder”, when being ambigiuos.

3.3.1 Ranks of the differentials

The maps \hat{d} in complex (3.1) can not be isomorphisms for generic dimensions of the spaces V . E.g., in case of a two-term complex,

$$0 \xrightarrow{\hat{d}_0} V_0 \xrightarrow{\hat{d}_1} V_1 \xrightarrow{\hat{d}_2} 0, \quad (3.13)$$

¹⁷If the T powers are not subsequent, i.e., $a_k = 0$ for some k , then problem (3.8) should be solved separately for the polynomials $\mathcal{F}'(T) = \sum_{k'=0}^{k-1} a_{k'}$ and $\mathcal{F}''(T) = \sum_{k+1}^n a_{k'}$ (such that $\mathcal{F}(T) = \mathcal{F}'(T) + \mathcal{F}''(T)$); this is a consequence of the positive coefficients requirement.

¹⁸In latter two cases we omit the inessential T power factor in \mathcal{F} by setting the smallest T power being equal zero.

the rank of the only non-zero map \hat{d}_1 must satisfy

$$\text{rank } \hat{d}_1 \equiv \dim \text{Im } V_1 \leq \min(\dim V_0, \dim V_1). \quad (3.14)$$

Starting from the next case of a three-term complex,

$$0 \xrightarrow{\hat{d}_0} V_0 \xrightarrow{\hat{d}_1} V_1 \xrightarrow{\hat{d}_2} V_2 \xrightarrow{\hat{d}_3} 0, \quad (3.15)$$

the nilpotency condition also becomes non-trivial, producing additional constraints. In particular, $\hat{d}_2 \hat{d}_1 = 0$ implies that

$$\text{Im } \hat{d}_1 \subset \ker \hat{d}_2 \Rightarrow \text{rank } \hat{d}_1 \equiv \dim \text{Im } \hat{d}_1 \leq \dim \ker \hat{d}_2 = \dim V_1 - \dim \text{Im } \hat{d}_2 \equiv \dim V_1 - \text{rank } \hat{d}_2, \quad (3.16)$$

i.e.,

$$\text{rank } \hat{d}_1 + \text{rank } \hat{d}_2 \leq \dim V_1, \quad (3.17)$$

apart from

$$\text{rank } \hat{d}_1 \leq \min(\dim V_0, \dim V_1), \quad \text{rank } \hat{d}_2 \leq \min(\dim V_1, \dim V_2), \quad (3.18)$$

similarly to the previous case.

Below we present the ranks of the differentials for the various cases of the corresponding division problem in the complexes (the correspondence is described in sec. 3.1.1) from tables (3.11–3.12) (omitting the trivial one-term case).

$\dim V_0 = v_0, \dim V_1 = v_1, \chi = v_0 - v_1$			
Case	$\chi > 0$	$\chi = 0$	$\chi < 0$
$\max \text{rank } \hat{d}_1$	v_0	$v_0 = v_1$	v_1
$\min \dim H_0 \subset V_0$	0	0	$-\chi$
$\min \dim H_1 \subset V_1$	χ	0	0

(3.19)

$\dim V_0 = v_0, \dim V_1 = v_1, \dim V_2 = v_2, \chi = v_0 - v_1 + v_2$						
Case	$\chi \leq 0$	$\chi > 0$				
		$v_0 \leq v_1 < v_2$	$v_2 \leq v_1 < v_0$	$v_1 < v_0, v_1 < v_2$	$v_0 \leq v_1, v_2 \leq v_1$	
$\text{rank } \hat{d}_1$	v_0	v_0	$v_1 - v_2$	$v_0 - p$	$v_1 - v_2$	v_0
$\text{rank } \hat{d}_2$	v_2	$v_1 - v_0$	v_2	$p - v_0 + v_1$	v_2	$v_1 - v_0$
$\dim H_0$	0	0	χ	$0 < v_0 - v_1 \leq p \leq v_0$	χ	0
$\dim H_1$	$-\chi$	0	0	0	0	0
$\dim H_2$	0	χ	0	$0 < v_2 - v_1 \leq \chi - p$	0	χ

(3.20)

3.3.2 Particular values of matrix elements

More detailed data include values of the separate matrix elements. To determine explicitly just several of the ones is sufficient to determine the ranks of the differentials, and hence the “minimal remainder”. For example,

$$\text{rank} \begin{pmatrix} k & k \end{pmatrix} = \begin{cases} 0, & k = 0 \\ 1, & k \neq 0 \end{cases}; \quad \text{rank} \begin{pmatrix} 1 & -1 & k \\ -1 & 1 & p \end{pmatrix} = \begin{cases} 0, & k + p = 0 \\ 1, & k + p \neq 0 \end{cases} \quad (3.21)$$

However, the general case is different, e.g.,

$$\forall k \text{ rank} \begin{pmatrix} 1 & k \end{pmatrix} = 1; \quad \forall k \text{ rank} \begin{pmatrix} 1 & -1 & k \\ -1 & 1 & 1-k \end{pmatrix} = 2; \quad \forall k \text{ rank} \begin{pmatrix} 1 & -1 & k \\ -1 & 1 & -k \end{pmatrix} = 1; \\ \forall k, p \text{ rank} \begin{pmatrix} 1 & 0 & k \\ 0 & 1 & p \end{pmatrix} = 2. \quad (3.22)$$

3.4 “Multilevel” division as a way to fix ambiguities

A further “improvement” consists in artificially splitting the initial division problem into two (or more) levels. Namely, suppose the original polynomial is given in form of the decomposition (the summation index Y running a given set of values)

$$\mathcal{F}(T) = \sum_Y \mathcal{F}_Y(T) C_Y(T). \quad (3.23)$$

Then, the division can be first performed for each $\mathcal{F}_Y(T)$ separately, and then for the linear combinations of the obtained remainders, namely

$$\text{I.} \quad \mathcal{F}_Y(T) = \mathcal{P}_Y(T) + (1+T)\mathcal{J}_Y(T). \quad (3.24)$$

$$\text{II.} \quad \mathcal{P}_1(T) \equiv \sum C_Y(T) \mathcal{P}_Y(T) = \mathcal{P}_{\text{II}}(T) + (1+T)\mathcal{J}_{\text{II}}(T). \quad (3.25)$$

The simplest example below illustrates how such “multilevel” division may fix an ambiguous remainder.

Let $\mathcal{G}(T) = 1+T$ and

Y	1	2
C_Y	1	T^2
\mathcal{F}_Y	$1+T$	1

(3.26)

so that $\mathcal{F}(T)$ admits two positive integer decompositions”, both with the monomial remainder,

$$\mathcal{F}(T) = \mathcal{F}_1 C_1 + \mathcal{F}_2 C_2 = 1 + T + T^2 = 1 + (1+T) \cdot T = T^2 + 1 \cdot (1+T). \quad (3.27)$$

From the standpoint of the “multilevel division, one decomposition is preferred, namely,

$$\text{I.} \quad \mathcal{F}_1 = 0 + 1 \cdot (1+T) \Rightarrow \mathcal{P}_1 = 0,$$

$$\mathcal{F}_2 = 1 + 0 \cdot (1+T) \Rightarrow \mathcal{P}_2 = 1.$$

$$\text{II.} \quad \mathcal{P} = \mathcal{P}_1 C_1 + \mathcal{P}_2 C_2 = 0 \cdot 1 + 1 \cdot T^2 = T^2 + 0 \cdot (1+T) \Rightarrow \boxed{\mathcal{P}_{\text{II}} = T^2}. \quad (3.28)$$

The suggested algorithm is motivated by the known properties of the knot polynomials to study, see [3] and sec. 4.3.

4 Lie algebra structure in the complex and its breaking

In this section, we return to the particular complex that arises in the context of knot invariants, associated with the Resolution hypercube (see sec. 2.3), and discuss in some further details the spaces at the vertices and the morphisms along the edges.

Namely, we slightly touch the topic of representation theory structures associated with the Resolution hypercube, and further with the constructed complex, and finally with the obtained knot invariants. Although at the moment we are not able neither present a closed construction, nor extract any practical output, we see at least two reasons for addressing to this subject.

First, the description of the spaces and differentials in the original KhR formalism [4, 22] refers to the representation theory (see ssec. 2.4–2.6 including the footnotes). In particular, it looks highly plausible the representation theory properties of the morphisms that determine their particular form to much extend.

Second, the known properties of the resulting knot invariants, they are the KhR invariants, as well as that of the closely related superpolynomials [10, 12], might have a natural representation theory interpretation. Namely, we imply the form these invariants take, when studied by means of either the differential expansion technique [28], or evolution method [25] (see sec. 4.3).

In this section, we use a number of representations theory notions and statements without any comments, assuming the reference to [38], whenever necessary.

4.1 Spaces in the resolution hypercube as representation spaces

The space $\mathcal{V}^* \subset V^{\otimes m}$ at the hypercube vertex $*$ is by construction a subspace of the tensor power of the representation space initially associated with the knot (the power m being the half number of the turning points on the knot diagram, see ssec. 2.4–2.5 including the footnote in p. 6).

An essential property of all the three operators ${}^*\mathcal{Z}$, \mathcal{Q} , and ${}^*\bar{\mathcal{Z}}$ defined respectively in (2.12), (2.13), and (2.16) is its commuting with all the algebra operators¹⁹, in particular,

$$A{}^*\bar{\mathcal{Z}} = {}^*\bar{\mathcal{Z}}A, \quad \forall A \in \mathfrak{g}, \quad * \in \{\circ, \bullet\}^n. \quad (4.1)$$

Relation (4.1) imply that

$$\forall x \in \mathcal{V}^* \left(\Leftrightarrow x = {}^*\bar{\mathcal{Z}}y \right) \Rightarrow Ax = {}^*\bar{\mathcal{Z}}(Ay) \in \mathcal{V}^*. \quad (4.2)$$

Hence, by definition,

- The space \mathcal{V}^* defined in sec. 4.1 is a representation space of the considered Lie algebra \mathfrak{g} ,

generally a **reducible** one.

4.2 Are the homology spaces representation spaces?

A non-trivial point of the construction is that

- The homology are **not** the representation spaces generally.

Indeed, by definition

$$\mathfrak{g} = \text{span}\{E_\alpha, F_\alpha, H_\alpha\}_{\alpha=1}^r. \quad (4.3)$$

Generally,

$$\hat{d}_k {}^*\bar{\mathcal{Z}} = {}^*\bar{\mathcal{Z}} \hat{d}_k \quad \text{and}, \quad \hat{d}_k E_\alpha = E_\alpha \hat{d}_k \alpha = \overline{1, r}, \quad k = \overline{1, n}, \quad (4.4)$$

but

$$\hat{d}_k F_\alpha \neq F_\alpha \hat{d}_k, \quad \text{and} \quad \hat{d}_k H_\alpha \neq H_\alpha \hat{d}_k. \quad (4.5)$$

Hence,

- The image has **always** the same grading as the original.
- The image of a descendent vector is **always** the corresponding descendent of the image.
- The image of the highest vector **not** generally a highest vector.

In particular, while the spaces \mathcal{V}_k are representation spaces of the Lie algebra \mathfrak{g} (i.e., $\mathfrak{g}(\mathcal{V}_k) \subset \mathcal{V}_k$), the subspaces $\bar{\mathcal{V}}'_m \subset \mathcal{V}_k$, $\bar{\mathcal{V}}'_m \text{Im } \hat{d}_{k-1}$, $\ker \hat{d}_k$, H_k must be invariant subspaces of the lowering, but not for the raising and Cartan operators, thus being **not** representation spaces generally ($E_\alpha(\mathcal{V}) \subset \mathcal{V}_k$ but $\mathfrak{g}(\mathcal{V}'_k) \not\subset \mathcal{V}'_k$).

Below we present two explicit examples of differentials with the properties (4.4) and, generally (4.5). A more involved example is given in App. C.

¹⁹As follows from the representation theory properties of the \mathcal{R} and \mathcal{Q} operators [38].

4.2.1 A toy example

Diagram (4.6) illustrates two possible maps (the differentials $\hat{d}^{(0)}$ and $\hat{d}^{(1)}$) of the first symmetric (type [2]) representation of the su_2 algebra. The differential $\hat{d}^{(0)}$ is the exact map, commuting with all the algebra operator. The differential $\hat{d}^{(1)}$ commutes only with the lowering operator E and has the non-trivial both the kernel and the co-kernel (the underlined terms in the first and second lines).

$$\begin{array}{ccccccc}
 & & \boxed{0} & \boxed{0} & \xrightarrow{E} & \boxed{x} & \boxed{x} \\
 & \xrightarrow{\hat{d}^{(0)}} & \boxed{0} & \xrightarrow{\hat{d}^{(1)}} & \boxed{x} & \downarrow & \boxed{x} \\
 \boxed{0} & \rightarrow & \boxed{0} & \rightarrow & \boxed{y \otimes x} & \rightarrow & \boxed{y \otimes Ex} \\
 & & & & & & \downarrow \\
 & & & & & \boxed{Ex} & \boxed{Ex} \\
 & & & & & \downarrow & \downarrow \\
 & & & & & \boxed{Ex} & \boxed{Ex} \\
 & & & & & \downarrow & \downarrow \\
 & & & & & \boxed{E^2x} & \boxed{\underline{E^2x}} \\
 & & & & & \downarrow & \downarrow \\
 & & & & & \boxed{E^2x} & \boxed{0} \\
 & & & & & \downarrow & \downarrow \\
 & & & & & \boxed{0} & \rightarrow \boxed{0}
 \end{array} \tag{4.6}$$

The gradings of the vectors are respectively equal to

$$\begin{array}{ccccccc}
 & \boxed{\emptyset} & \boxed{\emptyset} & \xrightarrow{E} & \boxed{\Delta} & \boxed{\Delta} & \rightarrow \boxed{\Delta-2} & \boxed{\Delta-2} \rightarrow \boxed{\Delta-4} & \boxed{\Delta-4} \rightarrow \boxed{\emptyset} \\
 & \xrightarrow{\hat{d}^{(0)}} & \boxed{\emptyset} & \xrightarrow{\hat{d}^{(1)}} & \boxed{\Delta} & \downarrow & \boxed{\Delta-2} & \downarrow & \boxed{\Delta-4} \\
 \boxed{\emptyset} & \rightarrow & \boxed{\emptyset} & \rightarrow & \boxed{\Delta+2} & \rightarrow & \boxed{\Delta} & \rightarrow & \boxed{\Delta-2} \rightarrow \boxed{\Delta-2} \rightarrow \boxed{\Delta-4} \rightarrow \boxed{\emptyset} \rightarrow \boxed{\emptyset}
 \end{array} \tag{4.7}$$

If now construct the generating function for the selected basis vectors of the mapped spaces, the differential $\hat{d} = \hat{d}^{(0)} + \hat{d}^{(1)}$ is then associated with the following positive integer decomposition (see sec. 2.8 for the definitions and comments),

$$\begin{aligned}
 \mathfrak{P} &= \mathcal{P}(q, T) + (1+T)\mathcal{Q}(q, T) = \\
 &= (1+q^2T)(q^\Delta + q^{\Delta-2} + q^{\Delta-4}) = \\
 &= (1+T)(q^\Delta + q^{\Delta-2} + q^{\Delta-4}) + (1+q^2T)(q^\Delta + q^{\Delta-2} + q^{\Delta-4}) = \\
 &= (1+T) \underbrace{(q^\Delta + q^{\Delta-2} + q^{\Delta-4})}_{\text{Im } \hat{d}^{(0)}} + q^{\Delta+2}T + (1+T) \underbrace{(q^\Delta + q^{\Delta-2})}_{\text{Im } \hat{d}^{(1)}} + q^{\Delta-4}, \\
 \mathcal{J} &= q^\Delta + 2q^{\Delta-2} + q^{\Delta-4}, \quad \mathcal{P} = q^{\Delta+2}T + q^{\Delta-4}.
 \end{aligned} \tag{4.8}$$

4.2.2 Relation to the real case

The simplest case appearing is the KhR construction is in fact reduced to the above example, by means of the correspondence between the $(N-1)$ -th symmetric ([$N+1$] type) representation of su_2 and the fundamental representation of su_{N+1} [38]. Namely, define $E = \sum_{\alpha=1}^N E_\alpha$. Then, the highest vector of the fundamental representation satisfy $F_\alpha x = 0$ for $\alpha = \overline{1, N}$ and $E^k x = E_k \dots E_2 E_1 x$ for $0 \leq k \leq N$ and $E^k x = 0$ for $k > N$.

The map corresponding to $\hat{d}^{(1)}$ in (4.6) for $N = 2$ then generally has the form

$$\begin{array}{ccccccc}
 F_\alpha x = 0, \alpha = \overline{1, r} & \boxed{0} & \rightarrow & \boxed{x} & \rightarrow & \boxed{E_1 x} & \rightarrow \dots \rightarrow \boxed{E_{n-1} \dots E_2 E_1 x} \rightarrow \boxed{0} \\
 \Delta y = 2y & \boxed{0} & \rightarrow & \boxed{y \otimes x} & \rightarrow & \boxed{y \otimes E_1 x} & \rightarrow \dots \rightarrow \dots \rightarrow \dots \rightarrow \dots \rightarrow \boxed{0}
 \end{array} \tag{4.9}$$

The simplest of the KhR maps just has the form of diagram (4.9), the grading being equal to [4]

$$\begin{array}{ccccccc}
 & \boxed{\emptyset} & \rightarrow & \boxed{N-1} & \rightarrow & \boxed{N-3} & \rightarrow \dots \rightarrow \boxed{N-5} \rightarrow \dots \rightarrow \boxed{-N+1} \rightarrow \boxed{\emptyset} \\
 & \downarrow & & \downarrow & & \downarrow & \dots \downarrow \\
 \boxed{\emptyset} & \rightarrow & \boxed{N-1} & \rightarrow & \boxed{N-3} & \rightarrow \dots \rightarrow \dots \rightarrow \dots \rightarrow \dots \rightarrow \boxed{\emptyset}
 \end{array} \tag{4.10}$$

4.3 Differential expansion and evolution method

4.3.1 Schematic sketch of the approaches

Now we wish to briefly outline two more (highly interrelated) approaches to the KhR (and super-) polynomials. Namely, we mean the *evolution method* [24, 25, 26] and the *differential expansion* [12, 25, 27, 28, 29] (see also discussion in [3], where, in particular, the relations between the variables used in different cited papers are explicitly written down). The both approaches do not ground on any rigourously formulated construction, yet being highly productive as computational tools (being in this sense much closer to the positive division approach considered here, than all the three ones to the original KhR approach). We relate this issue to this section minding to put the accent on the possible Lie group representation theory grounds of the named (by now mostly empiric) approaches. We complete the discussion by comparing the two approaches with the positive division approach (an interplay was already observed in [3]).

Both the evolution and the differential expansion methods suggest to study an entire knot family (either relatively general one, like all knots that are the closures of three-strand braids, or a rather special one, like the knots obtained from a given one by performing subsequently a certain transformation), and write the wanted knot invariant in the form

$$\text{Inv}^{\mathcal{K}}(q, T) = \sum_Y \text{Inv}_Y^{\mathcal{K}}(q, T) C_Y(q, T), \quad (4.11)$$

where Y is some summation label (e.g., just an integer, or a partition) running over a finite (and “small”) set, the quantities C_Y are treated as the common “expansion basis” for the knot family, while the “expansion” coefficients Inv_Y are either some (more or less) clear functions of some parameter(s) inside the family, or at least have a much simpler form than the resulting sum. Moreover, the “expansion basis” as standard consists of the products of some simple functions of an integer k (or, more generally, of a set of integers),

$$C_Y(q, T) = \frac{\prod_{k \in \phi \subset \mathbb{Z}} f^Y(k|q, T)}{\prod_{l \in \psi \subset \mathbb{Z}} g^Y(l|q, T)} \quad (4.12)$$

By construction, (4.11) for $T = -1$ must recover one of the known similar expansions for the HOMFLY polynomial (e.g., the character expansion [36, 33]). The factors in the “expansion basis” then often become certain representation theory quantities (e.g., the quantum dimensions of the irreducible representation spaces, see sec. 4.1), and the expansion factors typically take form of the *quantum numbers* $[n]_q \equiv \frac{q^n - q^{-n}}{q - q^{-1}}$ in the variable q . If this is the case, a typical “deformation” to the general T case consists in the substitution

$$f_k^Y(q, T = -1) = [n_k]_q \equiv \frac{q^{n_k} - q^{-n_k}}{q - q^{-1}} \quad \rightarrow \quad f_k^Y(q, T) = [n_k]_q \equiv \frac{q^{n_k} + q^{-n_k} T}{q + q^{-1} T}. \quad (4.13)$$

In many cases, the denominators cancel out, so that the answer takes form of a polynomial expanded over the ring generated by $\{(q^{n_k} + Tq^{-n_k})\}_{k \in \phi}$ (the generators are referred to as “differentials” in [28, 12, 25]).

4.3.2 An interplay with positive division method

The resulting “deformed” coefficients often appear to be in a simple relation with the first-level remainders from [3], while the “deformation” of the characters (4.13) coincides with the second-level reduction substitution (see sec. 3.4). (However, the general case is more complicated and yet far from being exhaustively studied).

From the Lie algebra standpoint discussed above, the primary deformation coupled to the minimal positive division for separate coefficients in (4.11) can be associated with the action of the “zero approximation” components of the differentials, which commute with all the Lie algebra generators (and hence, map each subspace of an irreducible representation to a subspace of isomorphic representation, which contributes to the same term in (4.11).), like $\hat{d}^{(0)}$ in fig. 4.6. In turn, the following second-level division (4.13) may correspond to the “symmetry breaking components”, like $\hat{d}^{(1)}$ in fig. 4.6.

5 Minimal positive division approach and the CohFT calculus

Now we turn to another, recently appeared point of view on the KhR calculus. We mean the CohFT field theory introduced in [14], namely the soliton counting technique developed in [1, 2]. We do not go into the field theory background, concentrating on necessary technical details instead. We mostly aim to compare this approach to the KhR invariants with the approach discussed above in ssec. 2–4.

5.1 Preliminary comments

5.1.1 CohFT diagram technique

Generally, the cohFT diagram is a knot diagram (see the definition in sec. 2.1), with a spin state (+ or $-$) put on each edge, and with the (several kinds of) solitons distributed over the crossings and turning points of the knot diagram. The various possible diagrams can be then organized into a graph, similar to resolution hypercube with various colorings in the vertices (sec. 2). However, the solitons (substituting the two colorings  and ) are distributed in different vertices non independently (see the particular examples below), hence the obtained graph has now a more complicated form, which we do not present explicitly.

In the original CohFT construction [14, 1, 2], the diagrams span certain vector spaces. These spaces further enter the complex, the differentials being given by their matrix elements on the various pair of the diagrams (thus the general idea is similar to that in the Khovanov [5, 18] and KhR [4, 22] constructions).

5.1.2 The selection rule for the CohFT matrix elements

It is essential that in the basis associated with the CohFT diagrams

- All the differentials in the constructed complex have the matrix elements equal either 0, or 1, or -1 , and each differential preserves an integer number associated with each diagram.

In other words, the CohFT diagrams enumerate the vectors of bases, analogous to the graded bases considered in (sec. 2.7). We recall that these bases (to be more profound, the properties of the differentials ensuring the ones are found) gave rise (in sec. 2.8) to the “positive integer decomposition” for the generating function, the generating function for the basis vectors in the homology spaces (which gives the wanted knot invariant) entering as the remainder of division of the original (polynomial) function on the certain polynomial. Hence, a similar decomposition can be written down in terms of the CohFT diagrams.

5.1.3 Types of the CohFT matrix elements and multilevel division

General considerations together with a case-study intuition result in further specification of the selection rules. In particular, the differentials preserving the initial spin state appear to be especially simple. Namely, a for a knot diagram having form of a braid closure, one can introduce the initial spin states as the distribution of signs over the strands at the bottom of the braid. Then

- The morphisms responsible for the transitions between the soliton diagrams with the same initial spin state commute with all the Lie algebra (of the gauge group) operators,

and hence

- The matrix element of the differential between all any pair of soliton diagrams with the same q grading and the T gradings differing by 1 is non-vanishing.

On the language of the minimal positive division this imply (see sec. 2.8) that, roughly speaking, the corresponding terms in the primary polynomial do **not** enter the remainder, whenever possible. The previous statement admits a rigorous formulation in the unambiguous division case (see sec. 2.8), namely,

- Only the first-level minimal remainders for the certain initial spin states (but generally not them all), if uniquely defined, enter the resulting remainder, which yields the knot invariant.

5.1.4 Our program

In this section, we present a straightforward way to calculate the explicit form of the generating function for all the CohFT diagrams. The way relies to the \mathcal{R} and \mathcal{Q} -matrix formalism (described in sec. 2.2), in principle being valid for any knot diagram, with any associated Lie algebra and its representations (see sec. 2.1). Here we study the case of the su_N algebra, the fundamental representation (when the KhR polynomial must be obtained), and positive braid closures as particular cases of the knot diagram (a general two-strand braid and particular cases of three-strand braids).

We subject then the obtained generating function to the minimal positive division described in sec. 3.

To determine the ambiguous remainder, we involve the idea of the “multilevel division from sec. 3.4. Namely, we write a decomposition of type (3.24), with Y running over the various distributions of the solitons over the turning points, expansion term Y generating all possible distributions of the solitons over the crossings in the relevant case.

Below we consider only the positive braids (all the crossings are \nearrow type). An \nearrow type crossing gives rise to a new set of solitons [1], as an unwanted complication on the current stage of the research.

5.2 Division algorithm for a generic two strand knot

5.2.1 The CohFT calculus in the two-strand case

Below we consider the particular case of a knot presented as a closure of a two strand positive braid with $n = 2k + 1$ crossings (all \nearrow type). A two-strand braid including negative (\nwarrow type) crossings as well is equivalent to a positive two-strand braid, modulo equivalence transformations (see App. A) and overall inversion²⁰ (if $\# \nearrow < \# \nwarrow$).

A cohFT diagram then can be presented as an $(n+2)$ -letter word. The first and the last letters stand for the solitons in the turning points²¹. The n letters stand for the solitons placed in the crossings, each of the letters being either \times , or $|$, or \ddagger . The distribution of the solitons must satisfy the certain constraints, so that not all words are allowed.

Below we treat these words as products of the non-commutative variables (the letters) and construct explicitly the generating function for all the allowed words.

Then search for an algorithm of presenting the obtained function as (3.6)-type decomposition with the wanted knot invariant as a remainder. For that we apply the “multi-level” division trick from sec. 3.4 with Y running over the pairs of values of the first and the last letters, $Y \in \{(\cap, \cap), (\cap, \cup), (\cup, \cap), (\cup, \cup)\}$.

We find that

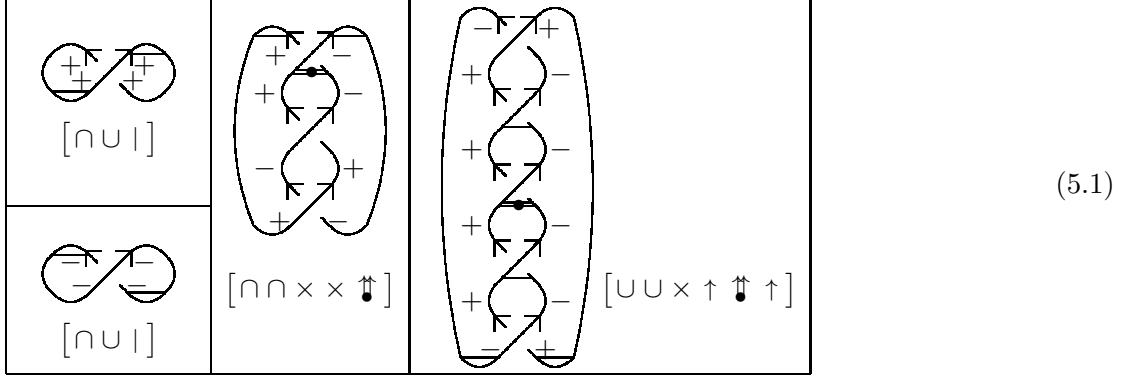
- the first-level remainders are unambiguous (see sec. 3.2) for any number of crossings;
- the second-level division can be performed algorithmically, by operating with the introduced non-commutative variables according to the certain “reduction rules”.

The corresponding “reduction rules” are explicitly formulated below.

²⁰The knot that is the closure of the resulting braid is then the mirror image of the original braid closure, the two knots generally being topologically distinct [6]. Accordingly, the inversion of all crossings affects non-trivially on the most of the knot

invariants, among them the Jones, HOMFLY, Khovanov, and KhR invariants we consider here [41]. The \nearrow type crossings desire considering already in the two strand case, yet we do not do it here.

²¹Two out of the four ones are taken into account, see the footnote in sec. 2.4.



5.2.2 Khovanov ($N = 2$) case

1. Calculate

$$\mathfrak{P}^{2,n}(q, T) = \mathfrak{R}_- \xi_- + \text{Tr} \left\{ \mathfrak{R}_\pm \begin{pmatrix} \xi_+ & \\ & \xi_- \end{pmatrix} \right\} \quad (5.2)$$

with

$$\mathfrak{R}_- = (q), \quad \mathfrak{R}_\pm = \begin{pmatrix} q & T \\ T & q + Tq^{-1} \end{pmatrix}, \quad \text{and} \quad \xi_- = \xi_+ + \xi_- . \quad (5.3)$$

2. Expand

$$\mathfrak{P}(\xi|q, T) = \sum_Y \mathfrak{P}^Y(q, T) \xi_Y, \quad Y \in \{++, --, +-, -+\}. \quad (5.4)$$

3. I.Reduce

$$\mathfrak{P}^Y(q, T) = \sum_k q^k \sum_{\vartheta=\vartheta_{Y,k}^{\min}}^{\vartheta=\vartheta_{Y,k}^{\max}} C_{\vartheta,u}^Y T^\vartheta \rightarrow \mathcal{P}_I^Y(q, T) \equiv \sum_k q^k T^{\vartheta_{Y,k}^{\min}}. \quad (5.5)$$

4. II.Reduce whenever possible

$$\begin{aligned} 1. \quad & q\xi_+ + q^{-1}T\xi_\pm \rightarrow 0. \\ 2. \quad & T^{2k+1}\xi_\pm + T^{2k+2}\xi_\mp \rightarrow 0. \end{aligned} \quad (5.6)$$

Do not reduce $T^{2k}\xi_\pm + T^{2k+1}\xi_\mp \rightarrow 0$!

5. Substitute $\xi_+ = q^2$, $\xi_- = q^{-2}$, $\xi_\pm = \xi_\mp = 1$.

6. The KhR polynomial equals

$\boxed{\text{Kh}^{[2,n]}(q, T) = q^{-2n} \mathfrak{P}_I(q, T)}.$

(5.7)

For each particular odd n the result reproduces the Khovanov polynomial for the two-strand knot with n crossings (torus knot $T[2, n]$) [7]. The particular case $n = 5$ is explicitly worked out below. (Even n correspond to the links, which we do consider here.)

5.2.3 KhR (generic N) case

1. Take expansion (5.4), reduced as in item 2 of sec. 5.2.2,

$$\mathfrak{P}_{\text{I}}(q, T) = \sum_Y \mathfrak{P}_{\text{I}}^Y(q, T) \xi_Y = \sum_Y \xi_Y \sum_k q^k T^{\vartheta_{Y,k}^{\min}}. \quad (5.8)$$

2. Substitute whenever possible

$$\begin{aligned} 1. \quad q^n \xi_{=} &+ q^{n-2} T \xi_{<} \rightarrow q^{N+n-1} [N]. \\ 2. \quad q^2 T^{2k+1} \xi_{<} &+ q^{-2} T^{2k+2} \xi_{>} \rightarrow T^{2k+1} (q^N + T q^{-N}) [N-1]. \end{aligned} \quad (5.9)$$

3. The KhR polynomial of the torus knot $T[2, n]$ equals

$$\boxed{\text{KhR}_N^{[2,n]}(q, T) = q^{-nN} \mathfrak{P}_{\text{II}}(N|q, T)}. \quad (5.10)$$

The result coincides with formula (4.55) from [3] (earlier proposed in [24] for the superpolynomials).

$$\text{KhR}_N^{[2,n]}(q, T) = q^{-(n-1)(N-1)} \left([N] + [N-1] (1 + q^{-2} T) \sum_{j=0}^{2j \leq n} q^{n-2j-4} T^{2j} \right). \quad (5.11)$$

5.2.4 Expressions for the primary polynomials as “deformed” expressions for the HOMFLY polynomials

Expression (5.2) is the result of deformation (2.23) of \mathcal{R} -matrix expression for the HOMFLY invariant (2.4), applied to the particular case of a two-strand braid closure as the knot diagram [36, 3]. Namely, $\mathfrak{R}_{=}$ and \mathfrak{R}_{\pm} are the blocks of “deformed” \mathcal{R} -matrices (2.11), up to the $(1+T)q$ entry reduced from the very beginning,

$$\mathfrak{R}_{=} = \mathfrak{R}_{ii}^{ii} = \frac{ii}{q \mid ii}, \quad 1 \leq i \leq N, \quad \mathfrak{R}_{\pm} = \left(\begin{array}{cc} \mathfrak{R}_{ij}^{ij} & \mathfrak{R}_{ij}^{ji} \\ \mathfrak{R}_{ji}^{ij} & \mathfrak{R}_{ji}^{ji} \end{array} \right) \cong \left(\begin{array}{cc|c} ij & ji & \\ 0 & T & \mid ij \\ T & q + T q^{-1} & \mid ji \end{array} \right), \quad 1 \leq i < j \leq N, \quad (5.12)$$

and ξ are the partial sums

$$\xi_{=} = \sum_{i=1}^N \mathcal{Q}_i^i, \quad \xi_{\pm} = \sum_{i < j=1}^N \mathcal{Q}_j^i, \quad \xi_{\mp} = \sum_{j < i=1}^N \mathcal{Q}_j^i, \quad (5.13)$$

separated from the entire contraction due to the independence of blocks (5.12) of i and j . Yet all the ξ must be treated as independent (of each other, as well as of q and T) variables in (5.2), unless all the reduction items are performed.

The factors in (5.7, 5.10) are the particular cases of the framing factors (skipped in (2.4), now restored; see App. A.2, here $w = n$, and $N = 2$ in (5.10)).

The substitutes in item 2 of sec. 5.2.3 are motivated by the identities for the corresponding addends in the HOMFLY polynomial, respectively,

$$q \xi_{=} + q^{-1} T \xi_{<} \xleftarrow{\text{HOMFLY}} q \frac{[2N]}{[2]} - q^{-1} \frac{[N][N-1]}{[2]} = q[N]^2 - [N][N-1] = q^N [N] \quad , \quad (5.14)$$

$$\left. \begin{aligned} & \\ & [N]^2 - \frac{[N][N-1]}{[2]} \end{aligned} \right\}$$

and

$$q^2 \xi_{>} + q^{-2} T \xi_{<} \xleftarrow{\text{HOMFLY}} (q^2 - q^{-2}) \frac{[N][N-1]}{[2]} = (q - q^{-1}) [N][N-1] = (q^N - q^{-N}) [N-1]. \quad (5.15)$$

5.2.5 Comparing the $N = 2$ and $N > 2$ cases

The reduction rules: $N = 2$ as a particular case of generic N . The level II reduction rules look out differently in the $N = 2$ (sec. 5.2.2, item 4) and generic N (sec. 5.2.3, item 2). Here we comment on their relation.

The first of the $N = 2$ rules, if presented in less detailed form $q^n\xi_+ + q^{n-2}T\xi_\pm \rightarrow q^{n-1}[2]$, with $\xi_+ \equiv \xi_+ + \xi_-$, just takes forms of the general rule, with $N = 2$ substituted.

The case of the second rule is different. Namely, the $N = 2$ rule (item 4 from sec. 5.2.2) explicitly contains the asymmetry between the odd and even T powers (see the comment in the bold type), the general N rule (item 3 from sec. 5.2.3) appear to be free of. In fact, there are several variants of the reduction rule for $N \leq 3$, all yielding the same remainder. In particular, one can take a straightforward generalization of the $N = 2$ rule, which is illustrated in tab. 5.16, 5.17.II for the $N = 2$ and $N = 3$ cases (compare with the rule in tab. 5.17.I, actually chosen in this case, and with a one more possibility in tab. 5.17.III).

$N = 2$	$\min(i, j)$	$q^{-1}T^3 + q^{-1}T^4 \not\rightarrow 0;$ $qT^2 + qT^3 \rightarrow 0, q^{-1}T^4 + q^{-3}T^5 \rightarrow 0.$			
$\max(i, j)$	0	$\cancel{qT^2}$ $q^{-1}T^3$ $\cancel{q^{-3}T^4}$ $q^{-5}T^5$			
1	$q \cdot q^{-1}$	q^3T^2 $\cancel{qT^3}$ $q^{-1}T^4$ $\cancel{q^{-3}T^5}$			

$N = 3$	$\min(i, j)$	I							
$\max(i, j)$	1 0	$q[2]T^2 (q + q^{-1}T) [3] \rightarrow qT^2[2] (q[2](q^3 + q^{-3}T)$							
2	$q^2 \cdot 1 \quad q^2 \cdot q^{-2}$	$qT^2 \times \begin{pmatrix} q^2 & \cancel{X} \\ \cancel{q}^{-2} & \end{pmatrix} \quad q^{-1}T^3 \times \begin{pmatrix} \cancel{q}^2 & \cancel{X} \\ q^{-2} & \end{pmatrix}$							
1	$1 \cdot q^{-2}$	$q^3T^2 \times \begin{pmatrix} q^2 & \cancel{X} \\ \cancel{q}^{-2} & \end{pmatrix} \quad qT^3 \times \begin{pmatrix} \cancel{q}^2 & \cancel{X} \\ q^{-2} & \end{pmatrix}$							
II									
$q^2T^2(q + q^{-1}T)[3] \rightarrow qT^2(q^2 + q^{-2}T)[2]$									
$qT^2(1 + T)[3] \rightarrow 0$									
$\cancel{qT^2} \times \begin{pmatrix} q^2 & 1 \\ q^{-2} & \end{pmatrix}$		$q^{-1}T^3 \times \begin{pmatrix} \cancel{q}^2 & 1 \\ q^{-2} & \end{pmatrix}$		$qT^2 \times \begin{pmatrix} \cancel{q}^2 & \cancel{X} \\ \cancel{q}^{-2} & \end{pmatrix}$					
$q^3T^2 \times \begin{pmatrix} q^2 & 1 \\ \cancel{q}^{-2} & \end{pmatrix}$		$\cancel{qT^3} \times \begin{pmatrix} q^2 & 1 \\ q^{-2} & \end{pmatrix}$		$q^{-1}T^3 \times \begin{pmatrix} \cancel{q}^2 & 1 \\ q^{-2} & \end{pmatrix}$					
III									
$q^3T^2 \times \begin{pmatrix} q^2 & 1 \\ \cancel{q}^{-2} & \end{pmatrix}$		$\cancel{qT^3} \times \begin{pmatrix} q^2 & 1 \\ q^{-2} & \end{pmatrix}$		$qT^3 \times \begin{pmatrix} \cancel{q}^2 & \cancel{X} \\ \cancel{q}^{-2} & \end{pmatrix}$					

In particular, one can see from the tables (5.17) that the odd-even asymmetry in fact presents in all versions of the reduction rules. However, the resulting remainder do not include a $\sim (1 + T)$ contribution in case $N \leq 3$. The difference is due to the additional q -power factors (below arranged in the triangle matrices), which account for various initial states giving rise to the same set of the soliton diagrams. Hence,

- The KhR polynomial of a two-stand knot is a minimal remainder for $N \leq 3$, unlike the Khovanov polynomial ($N = 2$) of the same knot.

To summarize,

- The $N = 2$ reduction rules are a particular case of the generic N reduction rules,

in the considered case of the two-strand knots. However, **this is not so for a general knot** because naive setting $N = 2$ in the (large N) the KhR polynomial does not always yield the correct Khovanov polynomial (compare the explicit examples in [22] with that in [7], and see e.g., in [3] for discussion).

5.2.6 The primary polynomial as the generating function for the soliton diagrams

Primary polynomial (5.2), subjected to the further “deformation”

$$\mathfrak{P} \rightarrow \hat{\mathfrak{P}} : \quad \mathfrak{R}_- \rightarrow \hat{\mathfrak{R}}_- = (\text{ } | \text{ }) , \quad \mathfrak{R}_\pm \rightarrow \hat{\mathfrak{R}}_\pm = \begin{pmatrix} 0 & \times & \times \\ \times & \uparrow & \mp \end{pmatrix} , \quad (5.18)$$

becomes the generating function for the soliton diagrams from [1]. Indeed, expression (5.18) is just the matrix notations of the diagram rules (A.33) from [1] (where one must substitute $q \rightarrow qT$, $[0] \rightarrow 1$, $[f_0] \rightarrow 1$, $[f_0 + 1] \rightarrow T$ and make the common factor $q^{-\frac{1}{2}}$ to obtain our formulas). The coefficient of each ξ in the resulting deformation of (5.4) then generates all the soliton diagrams with the given initial state, while the label of ξ runs over the various initial states, $Y \in \{ \begin{smallmatrix} + & - & + & - \\ + & - & + & - \end{smallmatrix} \}$ with $\pm \sim \begin{smallmatrix} + & - \\ - & + \end{smallmatrix}$, $\mp \sim \begin{smallmatrix} - & + \\ + & - \end{smallmatrix}$, and $= \sim \begin{smallmatrix} + & + \\ + & - \end{smallmatrix} \cup \begin{smallmatrix} - & - \\ - & + \end{smallmatrix}$ (the two coefficients identically coincide).

Explicit expressions for the coefficients in the primary polynomial. The coefficients in \mathfrak{P}_Y possesses explicit combinatorial formulas. In particular, the diagrams with the initial state \pm with w items of $\text{ } \times \text{ }$, b items of $\text{ } \times \text{ } \mp \text{ }$, and hence $n - w - b$ items of \times all contribute the \mathfrak{P}^\pm as the powers $q^w \times (q^{-1}T)^b T^{n-w-b} = q^{w-b} T^{n-w}$. Conversely, the coefficient of $q^k T^l$ in \mathfrak{P}^\pm gives the number of such diagrams with $w = n - l$ and $b = n - k + l$. One can see²² from the form of the matrix $\hat{\mathcal{R}}'_\pm$ that the \times crossings enter each contribution to the $\hat{\mathfrak{P}}_\pm$ only as the subsequent pairs $\text{ } \times \text{ } \times$, and the same is true for each contribution to the $\hat{\mathfrak{P}}$ but the two utmost entries always being equal \times . Hence, the coefficients in \mathfrak{P}_\pm are given by the numbers

$$\sharp \left(\text{ } \times \text{ } \times^c \text{ } | \text{ } ^w \text{ } \mp \text{ } ^b \right) = \nu_{n=w+b+2c|c,w,b} = \frac{n!!}{(w+b)!!c!} \frac{(w+b)!}{w!b!} , \quad (5.19)$$

which can be obtained from the expansion

$$f_n^\pm(x, y, z) = (2x^2 + (y+z)^2)^{\frac{n}{2}} = \sum \nu_{n|k,l,m} x^{2k} y^l z^m . \quad (5.20)$$

To explicitly obtain the T powers

$$f_n^\pm(T, q, q^{-1}T) = \left(2T^2 + (q + q^{-1}T)^2 \right)^{\frac{n}{2}} . \quad (5.21)$$

Similarly, the function

$$f_n^\mp(T, q, q^{-1}T) = T^2 f_{n-2}^\pm(T, q, q^{-1}T) \quad (5.22)$$

generates the coefficients in \mathfrak{P}_\pm .

Note that yet $\mathfrak{P}^Y \neq f^Y$, $Y \in \{\pm, \mp\}$, just the products of the q and T powers entering the \mathfrak{P} enter the f^Y with the same coefficients. The generating function that equals \mathfrak{P} identically has a more complicated form, which can be obtained by explicitly expressing the power $\hat{\mathfrak{R}}_\pm^n$ via the eigenvalues and the eigenvectors of the matrix.

Finally, $\mathfrak{P}_- = q^n$ corresponds to the only diagram $\hat{\mathfrak{P}}_-(| \text{ } |^n)$.

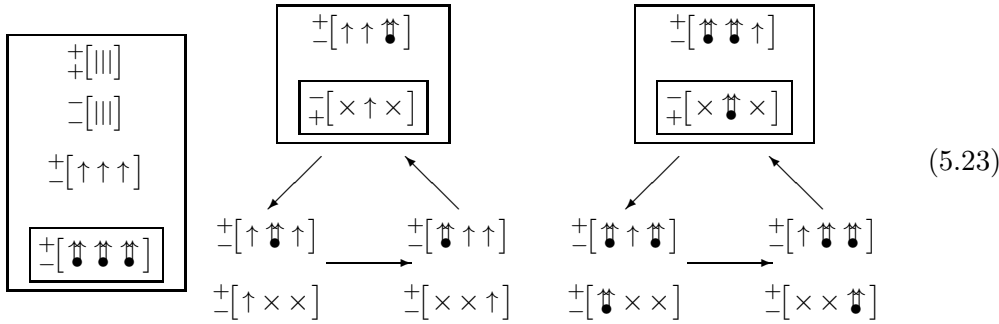
²²Because the $\hat{\mathfrak{R}}'$ has zero (11) entry, any two subsequent entries in a non-vanishing contribution to the matrix product must have the scripts equal (12)(21), or (12)(22), or (12)(21), or (21)(12), or (22)(22). Hence, (12) = \times entry always follows (21) = \times entry, and each (21) entry is always followed by (12) entry. By definition, \mathfrak{P}_\pm is obtained as (22) entry in the entire matrix product, hence each addend starts and ends either with entry (22) = $| \text{ } + \text{ } \mp \text{ }$, or with pair (21)(12) = $\text{ } \times \text{ } \times$. In turn, \mathfrak{P}_\mp equals to (11) entry, is the sum of the contributions starting with (12) entry and ending with (21) entry. The intermediate entries are the same as in \mathfrak{P}_\mp with $n \rightarrow n - 2$.

Involving the selection rules for the matrix elements in the division procedure. Deformation rule (5.18) sets a one-to-one correspondence between the monomials in primary polynomial (5.2) and the soliton diagrams. Then,

- The pairs of terms to omit in the reduction rules of sec. 5.2.2 correspond to the pairs of the soliton diagrams of [1] with the transition to each other allowed²³.

Covariance under the cyclic permutations. The suggested reduction rules are not invariant, rather covariant under the equivalence transformations of the knot diagram, namely under the cyclic shift of the crossings, the only one preserving a two-strand braid being such a one [6].

The table below illustrates the behaviour of the various soliton diagrams for n (the closure is the trefoil knot, 3_1 in [7]). Each diagram in the leftmost column is mapped to itself. The diagrams arranged in triangles are mapped to each other along the arrows. The diagrams arranged in the vertical pairs (mapped respectively) “cancel each other” due to the local rule $(\uparrow \uparrow) + (\times \times) \sim 0$ (not discussed here, see [1]).



5.2.7 Example: torus knot $T^{2,5}$.

The simplest example, when all the above items are non-trivial, is presented in tab. 5. Nothing essentially new happens for a two-stand knot with an arbitrary number of crossings.

The contributions to the first-level remainder are boxed. The contributions to the second-level remainder are double boxed. The terms marked by the same Roman numerals (the uppercase) “cancel each other” under the second level reduction. The lowercase labels mark the pairs of terms “cancelling” in the [1] variant of the reduction instead. The resulting remainders in the two cases contain different set of the soliton diagrams but are equal as polynomials in q and T , both yielding the correct value of the Khovanov polynomial for $T[2, 5]$ knot (5_1 in [7]).

5.3 The first-level division for particular three-strand knots

Now we turn to the first attempt to approach a more general case from the standpoint of the considered hybrid of the CohFT calculus and positive division technic.

In we restrict the following consideration to the case of Khovanov polynomials ($N = 2$), which already appears to be rather involved.

5.3.1 A draft of the three-strand reduction procedure

The below list almost generally follows the same the two-stand algorithm, yet differing at each step, the most of the steps being not completed at the moment.

²³In fact, the allowed transitions in [1] are related to a slightly different reduction rules, yet producing the same answer (see the explicit example below)

Table 5: Torus knot [2, 5], the soliton diagrams associated with all the terms the primary polynomial, in the first-level remainders (boxed), and in the Khovanov polynomial (double boxed).

\pm	$[5 \uparrow]$ $\boxed{q^5}$ $\mathbf{1}$					
\pm	$[5 \uparrow]$ $\boxed{q^5}$ $\mathbf{1}$					
\pm	I, i					
\pm	$[(5 \uparrow)]$ $\mathbf{1}$	$[(\uparrow 4 \uparrow)]$ $\boxed{5} = \frac{5!}{1!4!}$ $\boxed{q^5}$ \parallel $q^4 (q^{-1}T)$	$[(2 \uparrow 3 \uparrow)]$ $\mathbf{10} = \frac{5!}{2!3!}$ $\boxed{q^3T}$ \parallel $q^3 (q^{-1}T)^2 =$	$[(3 \uparrow 2 \uparrow)]$ $\mathbf{10}$ $\boxed{qT^2}$ \parallel $q^2 (q^{-1}T)^5$	$[(\uparrow 4 \uparrow)]$ $\mathbf{5}$ $\boxed{q^{-1}T^3}$ \parallel $q (q^{-1}T)^4$	$[(5 \uparrow)]$ $\mathbf{1}$ $\boxed{q^{-5}T^5}$ \parallel $(q^{-1}T)^5$
	I, i	II	ii	III	iii	
	$[(3 \uparrow \times \times)]$ $\mathbf{4}$ q^3T^2 \parallel $q^3 \cdot T^2$	$[(2 \uparrow \uparrow \times \times)]$ $\mathbf{12} = \frac{3!}{1!2!} \frac{(3+1)!}{3!1!}$ qT^3 \parallel $q^2 (q^{-1}T) \cdot T^2$	$[(\uparrow 2 \uparrow \times \times)]$ $\mathbf{12}$ $q^{-1}T^4$ \parallel $q (q^{-1}T)^2 \cdot T^2$	$[(3 \uparrow \times \times)]$ $\mathbf{4}$ $q^{-3}T^5$ \parallel $(q^{-1}T)^3 \cdot T^2$		
		$[(\uparrow 2 \times \times)]$ $\mathbf{3} = \frac{(2+1)!}{2!1!}$ $\star \quad qT^4$ \parallel $q \cdot T^2 \cdot T^2$	$[(\uparrow 2 \times \times)]$ $\mathbf{3}$ $\star \quad q^{-1}T^5$ \parallel $(q^{-1}T) \cdot T^2 \cdot T^2$			
		$[(\times (3 \uparrow) \times)]$ $\mathbf{1}$ $\boxed{q^3T^2}$ \parallel $T \cdot q^3 \cdot T$	$[(\times (2 \uparrow \uparrow) \times)]$ $\mathbf{3} = \frac{3!}{1!2!}$ $\boxed{qT^3}$ \parallel $T \cdot q^2 (q^{-1}T) \cdot T$	$[(\times (\uparrow 2 \uparrow) \times)]$ $\mathbf{3}$ $\boxed{q^{-1}T^4}$ \parallel $T \cdot q (q^{-1}T)^2 \cdot T$	$[(\times (3 \uparrow) \times)]$ $\mathbf{1}$ $\boxed{q^{-3}T^5}$ \parallel $T \cdot (q^{-1}T)^3 \cdot T$	
	ii	II	iii	III		
\mp		$[(\times (\uparrow) \times \times \times)]$ $\mathbf{2}$ qT^4 \parallel $T \cdot q \cdot T^2 \cdot T$	$[(\times (\uparrow \uparrow \times \times) \times)]$ $\mathbf{2}$ $q^{-1}T^5$ \parallel $T \cdot (q^{-1}T) \cdot T^2 \cdot T$			

1. For a three-strand braid $\mathcal{B} = (\mathcal{B}_i)_{i=1}^n$, $\mathcal{B}_i = 1, 2$ (fig. 4),

$$\mathfrak{P}^{\mathcal{B}}(q, T) = \sum_Y \text{Tr } \mathcal{Q}^Y(q) \prod_{i=1}^n \mathfrak{R}_{\mathcal{B}_i}^Y(q, T), \quad Y \in \{(000), (001), (011), (111)\}. \quad (5.24)$$

with

$$\mathcal{Q}^{(000)} = (\xi_{000}), \quad \mathcal{Q}^{(001)} = \text{diag}(\xi_{001} \xi_{010} \xi_{100}), \quad \mathcal{Q}^{(011)} = \text{diag}(\xi_{011} \xi_{101} \xi_{110}), \quad \mathcal{Q}^{(111)} = (\xi_{111}), \quad (5.25)$$

$$\mathfrak{R}_{-\mathcal{B}_i}^Y(q, T) = \mathfrak{R}_{\mathcal{B}_i}^Y(q^{-1}, T), \quad \text{and } \mathfrak{R}_{\mathcal{B}_i}^Y(q, T) \text{ for } \mathcal{B}_i > 0 \text{ given by (5.29).}$$

2. Expand

$$\mathfrak{P}(\xi|q, T) = \sum_Y \mathfrak{P}^Y(q, T) \xi_Y, \quad Y \in \{(000), (001), (011), (111)\}. \quad (5.26)$$

3. I.Reduce

$$\mathfrak{P}^Y(q, T) = (1 + T) \mathcal{J}^Y(q, T) + \mathcal{P}_{\min}^Y(q, T) \rightarrow \mathcal{P}_{\min}^Y(q, T), \quad (5.27)$$

to the residue containing the minimal possible number of q and T powers, **if the one is unique**.

4. II.Reduce further

$$\sum \mathcal{Q}^Y \mathcal{P}_{\min}^Y(q, T) \rightarrow ? \quad (5.28)$$

5. Substitute $\xi_{000} = q^3$, $\xi_{001} = \xi_{010} = \xi_{100} = q$, $\xi_{011} = \xi_{101} = \xi_{110} = q^{-1}$, $\xi_{111} = q^{-3}$.

6. The result must be proportional the the Khovanov polynomial of the knot $\mathcal{K} = \overline{\mathcal{B}}$ that is the closure of the braid \mathcal{B} (the factor is q^{-2w} with $w = \sum_{i=1}^N \mathcal{B}_i$, see sec. 5.2.4).

5.3.2 Explicit formulas for the three-strand (deformed) \mathcal{R} -matrices

From now on we switch to the notatitions $+$ $\rightarrow 0$ and $-$ $\rightarrow 1$, more natural for the \mathcal{R} -matrix formalism (especially if aiming for the generic N case). Just as in the two-strand case, we omit all the $q(1 + T)$ entries in the \mathcal{R} -matrices (as the sources of $\sim (1 + T)$ contributions newer entering the minimal remainders). All the needed matrices are explicitly given in the table below.

		I	II	III
To compute		The HOMFLY polynomial	The primary polynomial	The generating function
Y	k	$\begin{array}{c c} iii & \mathcal{R}_k^Y \\ \hline (q) & iii \end{array}$	\mathfrak{R}_k^Y	$\hat{\mathfrak{R}}_k^Y$
$(000), (111)$	$1, 2$	$, i = 0, 1$	(q)	$()$

(001)	1	$\begin{array}{c ccc} 001 & 010 & 100 & \\ \hline q & q - q^{-1} & -1 & \\ & -1 & & \end{array}$	$\begin{pmatrix} 001 \\ 010 \\ 100 \end{pmatrix}$	$\begin{pmatrix} q & q + q^{-1}T & T \\ T & & \end{pmatrix} \quad \begin{pmatrix} & \uparrow & \ddagger & \times \\ \times & & & \end{pmatrix}$	(5.29)
(011)	1	$\begin{array}{c ccc} 011 & 101 & 110 & \\ \hline q - q^{-1} & -1 & & \\ -1 & & & q \end{array}$	$\begin{pmatrix} 101 \\ 101 \\ 110 \end{pmatrix}$	$\begin{pmatrix} q + q^{-1}T & T \\ T & q \end{pmatrix} \quad \begin{pmatrix} & + & \ddagger & \times \\ \times & & & \end{pmatrix}$	(5.29)
(011)	2	$\begin{array}{c ccc} 011 & 101 & 110 & \\ \hline q & q - q^{-1} & -1 & \\ & -1 & & \end{array}$	$\begin{pmatrix} 011 \\ 101 \\ 110 \end{pmatrix}$	$\begin{pmatrix} q & q + q^{-1}T & T \\ T & & \end{pmatrix} \quad \begin{pmatrix} & & + & \ddagger & \times \\ \times & & & \end{pmatrix}$	(5.29)

5.4 The generating function for the three-strand soliton diagrams

Similarly to the two-strand case, expression (5.24) for the three-strand primary polynomial turns into a generating function for the soliton diagrams associated with the braid \mathcal{B} , if one substitutes $\hat{\mathfrak{R}}$ from col. **III** instead of \mathfrak{R} from col. **II** of (5.29), each monomial in the primary polynomial being then related to a certain soliton diagram.

We consider only the positive braids, i.e., all the crossings being the  type, and respectively all $\mathcal{B}_i > 0$. The form of a three strand braid is much more severely constraint by such assumption, than the form of a two strand braid (see sec. 5.2).

5.4.1 Guide to the experimental data

The three-strand positive braids with no more than 8 crossings, together with the knots or links being the closures, are enumerated in the App. D. Examples of the unique remainders, each term related to a set of soliton diagrams, are given in App. E, for the doubly twisted unknot diagram, presented as three-strand braid with 2 crossings (App. E.1), for all possible diagrams of the trefoil knot having form of three-strand braid with 4 crossings and providing the unique first level remainders (App. E.2), and for torus knot $T[3, 4]$ (8_{19} in [7]), presented a three-strand braid with 8 crossings²⁴.

²⁴This case desires a special interest, as the simplest case of the “thick” knot, i.e., with the continuous dependence of the KhR polynomial on N broken down (in this case, between $N = 2$ and $N = 3$) [3]

6 Further directions

We complete our presentation by enumerating the most natural directions for the following research.

1. **Systematic study of the $m \geq 3$ strand case.** Of course, the attempt presented in sec. 5.3 is just the first and a very naive one.
2. **Composite knots and links.** The knot invariants are commonly tabulated (e.g., in [7]) for the prime knots and links only. This is enough in many cases, including Jones, HOMFLY and Kauffman polynomial (in particular, the colored ones) [6], but not for the KhR and superpolynomials, neither even for the Khovanov polynomials. These invariants are thus far poorly studied even in the particular cases (a rare example can be found in [24]).
3. **Relation to the standard Khovanov-Rozansky construction.** It is highly mysterious that the KhR construction, apparently following just one of possible ways in many items (in particular, see the footnotes in the beginning of sec. 2.4 and in the beginning of 2.6), is discussed in the mathematical literature only in its original formulation [4, 22] literally. Any alternative (even not essentially different mathematically), if found, can be useful in one or another application. A detailed comparison of the \mathcal{R} -matrix construction, schematically described in sec. 2 and in sec. 4, with the rigorously formulated KhR construction, both on the general and the case study levels, provide some advances in this direction.
4. **Relation to the differential expansion.** This slightly concerned in sec. 4.3 issue definitely desires a systematic treatment.
5. **The problem of finite N .** The problem is in particular discussed in [3] and mentioned in sec. 5.2.5. The definition of the KhR polynomial [4] initially refers to same notions, as the \mathcal{R} -matrix definition of the HOMFLY polynomial, unless the differentials are introduced. In particular, the both invariants are associated with the su_N series of the Lie algebras (we tried to present this point mostly explicit in sec. 2). However, the HOMFLY invariants admit the most naive analytical continuation to arbitrary complex value of N , while the KhR polynomials admits one only for $N \leq N_0$ (with N_0 depending on the knot). The “phase transition” at $N = N_0$, which definitely happens at the level of homologies, is still not well studied and causes a wide interest.
6. **Higher representations and other groups?** Finally, the \mathcal{R} -matrix based approach possesses a highly inspiring property, already mentioned in sec. 2. Namely, it in principle can be extended to *arbitrary* Lie groups and representations, on the ground of the already exiting \mathcal{R} -matrix approaches to other knot invariants [6]. The colored (related to higher representations of the su_N Lie algebra) analogs of the KhR invariants are widely studied in various (often semi-empiric) ways [24, 25, 27, 28, 31, 9] (the list can be notably expanded). Yet the subject is even further from being exhausted, than in the case of ordinary KhR invariants. In particular, and even exact definition of the colored KhR invariants (superpolynomials) encounters with essential difficulties, in particular, discussed in [30, 32] (the second paper concerns a possible extension of the cabling approach [42] to the superpolynomials).

Acknowledgements

The author is deeply indebted to A. Yu. Morozov for scientific direction of this work, and to D. Galakhov and I. Danilenko for long inspiring discussions and patent explanations. The author also thanks G. Aminov, M. Bishler, Y. Zenkevich, And. Morozov, and Sh. Shakirov for valuable comments to the draft, and all participant of the Mathematical physics group seminar for interest to this work. The author is grateful to the secretary of the mathematical physics group E. S. Syslova, who makes possible the work of the author and his colleagues for many years.

This work was funded by the Russian Science Foundation (grant N 16-12-10344).

References

- [1] Galakhov D., Moore G. — arXiv : hep-th/1607.04222.
- [2] Galakhov D. — arXiv : hep-th/1702.07086.
- [3] Anokhina A., Morozov A. // JHEP. — 2014. — Vol. 07, no. 063. — arXiv : hep-th/1403.8087.
- [4] Khovanov M., Rozansky L. Matrix factorizations and link homology // Fund. Math. — 2008. — Vol. 199. — P. 1–91. — arXiv : math.QA/0401268.
- [5] Khovanov M. A categorification of the Jones polynomial // Duke Math. J. — 2000. — Vol. 101. — P. 359–426.
- [6] Kauffman L. H. The interface of knots and physics. — Singapore : World Scientific, 2001. — P. 788.
- [7] Bar-Natan D., Scott M., et al. The Knot Atlas. — URL: <http://katlas.org> (online; accessed: 22.10.17).
- [8] Morozov And., Sleptsov A., et al. The knotbook. — URL: www.knotbook.org (online; accessed: 22.10.17).
- [9] Gukov Sergei, Khovanov Mikhail, Walcher Johannes. Physics and Mathematics of Link Homology. — Providence : AMS, 2016. — P. 177.
- [10] Gukov S., Schwarz A., Vafa C. Khovanov-Rozansky homology and topological strings // Lett. Math. Phys. — 2005. — Vol. 74. — P. 53–74. — arXiv : hep-th/0412243.
- [11] Rasmussen Jacob. — 2006. — arXiv : math.GT/0607544.
- [12] Dunfield N. M., Gukov S., Rasmussen J. The superpolynomial for knot homologies // Experimental Math. — 2006. — Vol. 15. — P. 129–159. — arXiv : math/0505662.
- [13] Gorsky Eugene, Lewark Lukas // Experimental Mathematics. — 2015. — Vol. 24. — P. 162–174. — arXiv : math.GT/1404.0623.
- [14] Gaiotto D., Witten E. — arXiv : hep-th/1106.4789.
- [15] Schwarz A. S. New topological invariants arising in the theory of quantized fields // International Topological Conference. — Vol. 2. — Baku : Institute of Mathematics and Mechanics of the Azerbaijan Academy of Sciences of USSR, 1987.
- [16] Witten E. Quantum field theory and the Jones polynomial // Comm. Math. Phys. — 1989. — Vol. 121. — P. 351–399.
- [17] Witten E. Gauge theories and integrable lattice models // Nucl. Phys. — 1989. — Vol. B322. — P. 629–697.
- [18] Bar-Natan D. On Khovanov’s categorification of the Jones polynomial // Algebr. Geom. Topol. — 2002. — Vol. 2. — P. 337–370. — arXiv : math.QA/0201043.
- [19] Dolotin V., Morozov A. Introduction to Khovanov homologies. I. Unreduced Jones superpolynomial // JHEP. — 2013. — Vol. 1301, no. 065. — arXiv : hep-th/1208.4994.
- [20] Dolotin V., Morozov A. Introduction to Khovanov homologies. II. Reduced Jones superpolynomials // J. Phys.: Conf. Ser. — 2013. — Vol. 411, no. 012013. — arXiv : hep-th/1209.5109.
- [21] Nawata Satoshi, Oblomkov Alexei. Proceedings of.
- [22] Carqueville N., Murfet D. Computing Khovanov-Rozansky homology and defect fusion // Algebr. Geom. Topol. — 2014. — Vol. 14. — P. 489–537. — arXiv : hep-th/1108.1081.

[23] Dolotin V., Morozov A. Introduction to Khovanov homologies. III. A new and simple tensor-algebra construction of khovanov-rozansky invariants // *Nucl. Phys.* — 2014. — Vol. B878. — P. 12–81. — arXiv : hep-th/1308.5759.

[24] Superpolynomials for torus knots from evolution induced by cut-and-join operators / P. Dunin-Barkowski, A. Mironov, A. Morozov et al. // *JHEP*. — 2013. — Vol. 03, no. 021. — arXiv : hep-th/1106.4305.

[25] Mironov A., Morozov A., Morozov An. Evolution method and “differential hierarchy” of colored knot polynomials // *AIP Conf. Proc.* — 2013. — Vol. 1562. — arXiv : hep-th/1306.3197.

[26] Evolution method and HOMFLY polynomials for virtual knots / L. Bishler, A. Morozov, And. Morozov, Ant. Morozov // *Int. J. of Mod. Phys.* — 2015. — Vol. A30, no. 1550074. — arXiv : hep-th/1411.2569.

[27] Gorsky E., Gukov S., Stosic M. Quadruply-graded colored homology of knots. — 2014. — arXiv : math.QA/1304.3481.

[28] S.Arthamonov, A.Mironov, A.Morozov // *Theor.Math.Phys.* — 2014. — Vol. 179. — P. 509–542. — arXiv : hep-th/1306.5682.

[29] Kononov Ya., Morozov A. // *JETP Letters*. — 2015. — Vol. 101. — P. 831–834. — arXiv : hep-th/1504.07146.

[30] Khovanov Mikhail // *Knot theory and its Ramifications*. — 2005. — Vol. 14, no. 1. — P. 111–130. — arXiv : math.QA/0302060.

[31] Nawata S., Ramadevi P., Zodinmawia // *JHEP*. — 2014. — Vol. 1401, no. 126. — arXiv : hep-th/1310.2240.

[32] Danilenko I. — arXiv : hep-th/1405.0884.

[33] Turaev V. G. The Yang-Baxter equation and invariants of links // *Invent. Math.* — 1988. — Vol. 92. — P. 527–533.

[34] Reshetikhin N. Yu., Turaev V. G. Ribbon graphs and their invariants derived from quantum groups // *Commun. Math. Phys.* — 1990. — Vol. 127. — P. 1–26.

[35] Morozov A., Smirnov A. Chern-simons theory in the temporal gauge and knot invariants through the universal quantum R-matrix // *Nucl. Phys.* — 2010. — Vol. B835. — P. 284–313. — arXiv : hep-th/1001.2003.

[36] Mironov A., Morozov A., Morozov And. Character expansion for HOMFLY polynomials. II. fundamental representation. up to five strands in braid // *JHEP*. — 2012. — Vol. 03. — arXiv : hep-th/1112.2654.

[37] Anokhina A. On R-matrix approaches to knot invariants. — 2014. — arXiv : hep-th/1412.8444v2.

[38] Klimyk A., Schmüdgen K. Quantum groups and their representations. — Berlin : Springer, 2012. — P. 552.

[39] Groups Loop. Andrew Pressley and Graeme Segal. — Oxford : Clarendon Press, Oxford Mathematical Monographs, 1988. — P. 316.

[40] S.I. Gelfand, Yu.I. Manin. Homological Algebra. — Berlin : Springer, 1994. — P. 222.

[41] Sergei Gukov Marko Stosic // *Geometry & Topology Monographs*. — 2012. — Vol. 18. — P. 309–367. — arXiv : hep-th/1112.0030.

[42] A.Anokhina, An.Morozov // *Theor.Math.Phys.* — 2014. — Vol. 178. — P. 1–58. — arXiv : hep-th/1307.2216.

A Basic properties of the special point operators

Continuous space transformations and transformations of the knot diagram. To treat the knot \mathcal{K} up to arbitrary continuous space transformations is equivalent to treating the knot diagram $\mathcal{D}(\mathcal{K})$ up arbitrary continuous plane transformations, coupled to a certain group of transformations affecting the crossings. The group is generated by the three *Reidemeister moves* (fig. A.1,A.2) [6]. Wherein, a general continuous plane transformation can be presented as a composition of a transformation preserving the number and types of the turning points and transformation (that changes) from one more finitely generated group [6].

Topological invariance constraints on the crossing and turning point operators. Contraction (2.4) by construction ignores the continuous, turning point-preserving planar transformations. Hence, the obtained quantity is a topological invariant (ignores the entire group of the transformations representing the continuous space transformations, see above) provided that the operators \mathcal{R} and \mathcal{Q} satisfy a finite set of constraints explicitly presented below.

A.1 Constraints on the \mathcal{R} -matrices

Transformations in fig. A.1 are the planar projections of the continuous space transformations affecting on the knot diagram as the generators of the vertices changing subgroup (of the entire equivalence transformations group). The corresponding space constraints on the vertex (\mathcal{R}) operators are below each figure.

$$\begin{array}{ccc}
 \begin{array}{c} k \\ \nearrow \\ a \\ \curvearrowleft \\ i \end{array} \begin{array}{c} l \\ \nearrow \\ b \\ \curvearrowleft \\ j \end{array} & = & \begin{array}{c} k \\ \nearrow \\ i \\ \curvearrowleft \\ j \end{array} \\
 \begin{array}{c} \bar{\mathcal{R}}_{ab}^{ji} \mathcal{R}_{kb}^{al} \\ = \delta_k^i \delta_l^j \end{array} & &
 \end{array}
 \quad
 \begin{array}{ccc}
 \begin{array}{c} k \\ \nearrow \\ m \\ \curvearrowleft \\ p \end{array} \begin{array}{c} l \\ \nearrow \\ b \\ \curvearrowleft \\ c \\ \curvearrowleft \\ i \end{array} & = & \begin{array}{c} m \\ \nearrow \\ a \\ \curvearrowleft \\ b \\ \curvearrowleft \\ c \\ \curvearrowleft \\ j \end{array} \\
 \begin{array}{c} {}^* \mathcal{R}_{jc}^{ia} {}^* \mathcal{R}_{cm}^{pb} {}^* \mathcal{R}_{ak}^{bl} \\ = {}^* \mathcal{R}_{ia}^{pb} {}^* \mathcal{R}_{jc}^{bl} {}^* \mathcal{R}_{cm}^{ak}, \quad * \in \{+, -\} \end{array} & &
 \end{array}$$

A.2 Relations between the \mathcal{R} and \mathcal{Q} -matrices

Extremum point operators. The considered approach to the knot invariants requires not only to project the knot on a plane, but for selecting a direction in the plane as well [34, 6, 35]. As a result, one must treat the turning points as two-valent vertices on the knot diagram (apart from the crossings treated as four-valent vertices), of the four kinds: , , , .

The equivalence transformations of the knot diagram changing the number of the turning points must be then considered separately. These transformations form a finite subgroup, the generators giving rise to the relations between different \mathcal{Q} , as well as between \mathcal{R} and \mathcal{Q} matrices (both presented below).

$$\begin{array}{ccc}
 \begin{array}{c} k \\ \curvearrowleft \\ j \\ \curvearrowleft \\ i \end{array} & \cong & \begin{array}{c} k \\ \curvearrowleft \\ i \end{array} \\
 \begin{array}{c} \leftarrow \mathcal{Q}_j^i \mathcal{Q}_k^j \\ = \delta_k^i \end{array} & &
 \end{array}
 \quad
 \begin{array}{ccc}
 \begin{array}{c} i \\ \curvearrowleft \\ j \\ \curvearrowleft \\ k \end{array} & \cong & \begin{array}{c} i \\ \rightarrow \\ k \end{array} \\
 \begin{array}{c} \mathcal{Q}_j^i \mathcal{Q}_k^j \\ = \delta_k^i \end{array} & &
 \end{array}
 \tag{A.1}$$

$$\begin{array}{ccc}
 \begin{array}{c} l \\ \nearrow \\ k \\ \curvearrowleft \\ i \\ \curvearrowleft \\ j \end{array} & \cong & \begin{array}{c} p \\ \curvearrowleft \\ k \\ \nearrow \\ l \\ \curvearrowleft \\ i \\ \curvearrowleft \\ j \end{array} & \cong & \begin{array}{c} \uparrow \\ i \\ k \end{array} \\
 \begin{array}{c} \leftarrow \mathcal{Q}_p^j \mathcal{Q}_l^p \mathcal{R}_{kl}^{ij} \\ = \leftarrow \mathcal{Q}_p^j \mathcal{Q}_l^p \mathcal{R}_{kl}^{ij} = \kappa \delta_k^i \end{array} & & & &
 \end{array}
 \tag{A.2}$$

The factor κ here depends on the particular solutions of (A.1) for the \mathcal{R} operators. In particular, $\kappa = q^{-N}$ for solution (2.6).

Framing factor. Factor one can set $\varkappa = 1$ by rescaling the $\mathcal{R} \rightarrow \varkappa \mathcal{R}$, making use of constraints (A.1) being homogeneous. Yet, this is not usually done, because the resulting \mathcal{R} explicitly depends on the chosen Lie algebra su_N via N . Contraction (2.4) is then topologically invariant, after multiplied on q^{-wN} for the knot diagram with the algebraic number of crossings being $w \equiv \# \times - \# \times$.

Types of crossings in presence of the selected direction. As the second consequence of the direction selected, one must consider no longer two (\times and \times) kinds of crossings, but four variants of each one differing by inverting of one arrow (thus 8 kinds overall). The topological invariance then requires for introducing 8 distinct operators, related to each other via the extremum point operators. The corresponding relations are given below.

$$\begin{array}{c} k \\ \swarrow \quad \searrow \\ l \quad i \end{array} \cong \begin{array}{c} \nearrow \quad \searrow \\ \swarrow \quad \nwarrow \end{array} \cong \begin{array}{c} \nearrow \quad \searrow \\ l' \quad k \\ \swarrow \quad \searrow \\ i \quad j' \\ \searrow \quad \swarrow \\ j \end{array} \quad \begin{array}{c} \leftarrow \mathcal{Q}_{j'}^j \leftarrow \mathcal{Q}_l^{l'} + \mathcal{R}_{k'l'}^{i'j'} \end{array} \quad (A.3)$$

$$\begin{array}{c} i \\ \nearrow \quad \nearrow \\ j \quad k \end{array} \cong \begin{array}{c} \nearrow \quad \nearrow \\ \swarrow \quad \searrow \end{array} \cong \begin{array}{c} \nearrow \quad \nearrow \\ l' \quad k' \\ \swarrow \quad \searrow \\ i \quad j \\ \searrow \quad \swarrow \\ j \end{array} \quad \begin{array}{c} \rightarrow \mathcal{Q}_{i'}^i \rightarrow \mathcal{Q}_k^{k'} + \mathcal{R}_{k'l'}^{i'j'} \end{array} \quad (A.4)$$

$$\begin{array}{cccc} \begin{array}{c} + \\ \mathcal{R}_{kl}^{ij} \end{array} & \begin{array}{c} l \nearrow \quad k \\ \swarrow \quad j \end{array} & \begin{array}{c} - \\ \mathcal{R}_{kl}^{ij} \end{array} & \begin{array}{c} k \nearrow \quad l \\ j \nearrow \quad i \end{array} \\ \parallel & & \parallel & \\ \begin{array}{c} \leftarrow \mathcal{Q}_{j'}^j \leftarrow \mathcal{Q}_l^{l'} \rightarrow \mathcal{Q}_{i'}^i \rightarrow \mathcal{Q}_k^{k'} + \mathcal{R}_{k'l'}^{i'j'} \end{array} & \begin{array}{c} j \nearrow \quad i \\ k \swarrow \quad l \end{array} & \begin{array}{c} \leftarrow \mathcal{Q}_{i'}^i \leftarrow \mathcal{Q}_k^{k'} \rightarrow \mathcal{Q}_{j'}^j \rightarrow \mathcal{Q}_l^{l'} - \mathcal{R}_{k'l'}^{i'j'} \end{array} & \begin{array}{c} i \nearrow \quad j \\ l \swarrow \quad k \end{array} \\ & & & \\ \begin{array}{c} \leftarrow \mathcal{Q}_{j'}^j \leftarrow \mathcal{Q}_l^{l'} + \mathcal{R}_{kl}^{ij'} \end{array} & \begin{array}{c} i \nearrow \quad l \\ j \nearrow \quad k \end{array} & \begin{array}{c} \leftarrow \mathcal{Q}_{i'}^i \leftarrow \mathcal{Q}_k^{k'} - \mathcal{R}_{k'l'}^{i'l} \end{array} & \begin{array}{c} j \nearrow \quad k \\ i \swarrow \quad l \end{array} \\ \parallel & & \parallel & \\ \begin{array}{c} \rightarrow \mathcal{Q}_{i'}^i \rightarrow \mathcal{Q}_k^{k'} + \mathcal{R}_{k'l'}^{i'j} \end{array} & \begin{array}{c} k \nearrow \quad j \\ l \swarrow \quad i \end{array} & \begin{array}{c} \rightarrow \mathcal{Q}_{k'}^k \rightarrow \mathcal{Q}_l^{l'} - \mathcal{R}_{kl}^{ij'} \end{array} & \begin{array}{c} l \nearrow \quad i \\ k \swarrow \quad j \end{array} \end{array} \quad (A.5)$$

The commutation relations. Finally, the both \mathcal{R} operators commute with the tensor squares of all the four \mathcal{Q} operators (we skip the corresponding equivalence transformations),

$$\mathcal{Q}_{i'}^i \mathcal{Q}_{j'}^j \mathcal{R}_{kl}^{ij'} = \mathcal{Q}_k^{k'} \mathcal{Q}_l^{l'} \mathcal{R}_{k'l'}^{ij}, \quad * \in \{+, -\}, \quad \times \in \{\leftarrow \curvearrowright, \curvearrowright \rightarrow, \leftarrow \curvearrowleft, \curvearrowleft \rightarrow\}. \quad (A.6)$$

Relations (A.6) follow from relations (A.2, A.1) and provide the vertical qualities in relations (A.5).

Freedom in the definition of the turning point operators. In fact, topological invariance constraints (A.2, A.1) fix only the pairwise products. Any four \mathcal{Q} operators satisfying the equations below yield the same value of the knot invariant [34, 6, 35]. In particular, one select these operators as in (2.7), the two ones being the unity operators, the related turning point can being ignored (just as we do through the text).

A.3 Properties of the particular solution

The ${}^+\mathcal{R}$ - and ${}^-\mathcal{R}$ -operators given by particular solution (2.6) of the topological invariance constraints satisfy the additional, so called *skein* relations, namely [33, 38],

$$\begin{aligned} l \nearrow \begin{matrix} k \\ i \\ j \end{matrix} - k \nearrow \begin{matrix} l \\ j \\ i \end{matrix} &= (q - q^{-1}) \begin{matrix} k \\ i \\ j \end{matrix} \\ {}^+\mathcal{R}_{kl}^{ij} - {}^-\mathcal{R}_{kl}^{ij} &= (q - q^{-1}) \delta_k^i \delta_l^j. \end{aligned} \quad (\text{A.7})$$

These relations together with (A.1) lead to the characteristic equations

$$({}^+\mathcal{R} - q)({}^+\mathcal{R} + q^{-1}) = 0, \quad ({}^-\mathcal{R} - q^{-1})({}^-\mathcal{R} + q) = 0 \quad (\text{A.8})$$

implying that each of the crossing operators has just two distinct eigenvalues, q and $(-q^{-1})$ for ${}^+\mathcal{R}$, and q^{-1} and $(-q)$ for ${}^-\mathcal{R}$.

The \mathcal{R} and \mathcal{Q} having form (2.6,2.7), thus the former once satisfying (A.8) corresponds to the space V related to each edge of the knot diagram being the fundamental representation space for the su_N . Hence, this choice of V is essential for the entire construction, which in all variants [5, 4, 23, 3] heavily relies on decomposition (2.8) following from (A.8). Yet, the explicit \mathcal{R} -matrix form of (2.8) in principle lets for a generalization, based on the general form of the characteristic equation, explicitly known for arbitrary Lie groups and their representations [38].

B The “graded” basis respected by the differentials

Here we describe in more details of the “grades” basis, selected in sec. 2.7 in the Khovanov complex and used in 2.8 to derive the Positive integer decomposition for the generating function $\mathfrak{P}(q, T)$.

Recall that by definition

$$\mathcal{V}_k = \text{Im } \hat{d}_k \oplus \text{coIm } \hat{d}_{k+1} \oplus H_k \Leftrightarrow x = \hat{d}_k y + z + h, \quad \forall x \in \mathcal{V}_k. \quad (\text{B.1})$$

(In particular, $x \in \text{coIm } \hat{d} \Leftrightarrow \hat{d}x \neq 0$).

To simplify the following formulas we introduce the grading operator $\hat{\Delta}$ such that ${}^*\bar{\mathcal{Z}} = q^{\hat{\Delta}}$. Then, one can chose in the space \mathcal{V}_k the basis composed of three groups of the vectors

$$\begin{aligned} \left\{ y_{k,i} : \hat{d}_{k+1} y_{k,i} \neq 0 \right\}_{i=1}^{\dim \text{Im } \hat{d}_{k+1}} \cup \left\{ z_{k,i} = \hat{d}_k y_{k-1,i} \right\}_{i=1}^{\dim \text{Im } \hat{d}_k} \cup \left\{ h_{k,i} \right\}_{i=1}^{\dim \mathcal{V}_k - \dim \text{Im } \hat{d}_k - \dim \text{Im } \hat{d}_{k+1}}, \\ \hat{\Delta} y_{k,i} = \Delta_{k,i} y_{k,i} \quad \hat{\Delta} z_{k,i} = \Delta_{k-1,i} z_{k,i} \quad \hat{\Delta} h_{i,k} = \Delta'_{i,k} h_{i,k} \end{aligned} \quad (\text{B.2})$$

The groups are selected subsequently for the all spaces \mathcal{V}_k ($k = \overline{0, n}$) in the complex, the transition $k \rightarrow k+1$ being performed as follows. First, the vectors $\left\{ z_{k,i} = \hat{d}_k y_{k-1,i} \right\}_{i=1}^{\dim \text{Im } \hat{d}_k}$ are linearly independent and have definite grading by construction. Then, the vectors z by definition span the space $\text{Im } \hat{d}_k$, which is an invariant subspace of the grading operator $\hat{\Delta}$ (because $x = \hat{d}_k y \Rightarrow \hat{\Delta}x = \hat{d}_k \Delta y \in \text{Im } \hat{d}$ for any $y \in \hat{d}_k$), and, similarly, so does the factor space $\text{coIm } \hat{d}_k \equiv \mathcal{V}_k / \text{Im } \hat{d}_k$. The latter one contains then the basis of the $\hat{\Delta}$ eigenvectors,

$$\left\{ x_{k,i} \in \text{coIm } \hat{d}_k \right\}_{i=1}^{\dim \mathcal{V}_k - \dim \text{Im } \hat{d}_k}. \quad (\text{B.3})$$

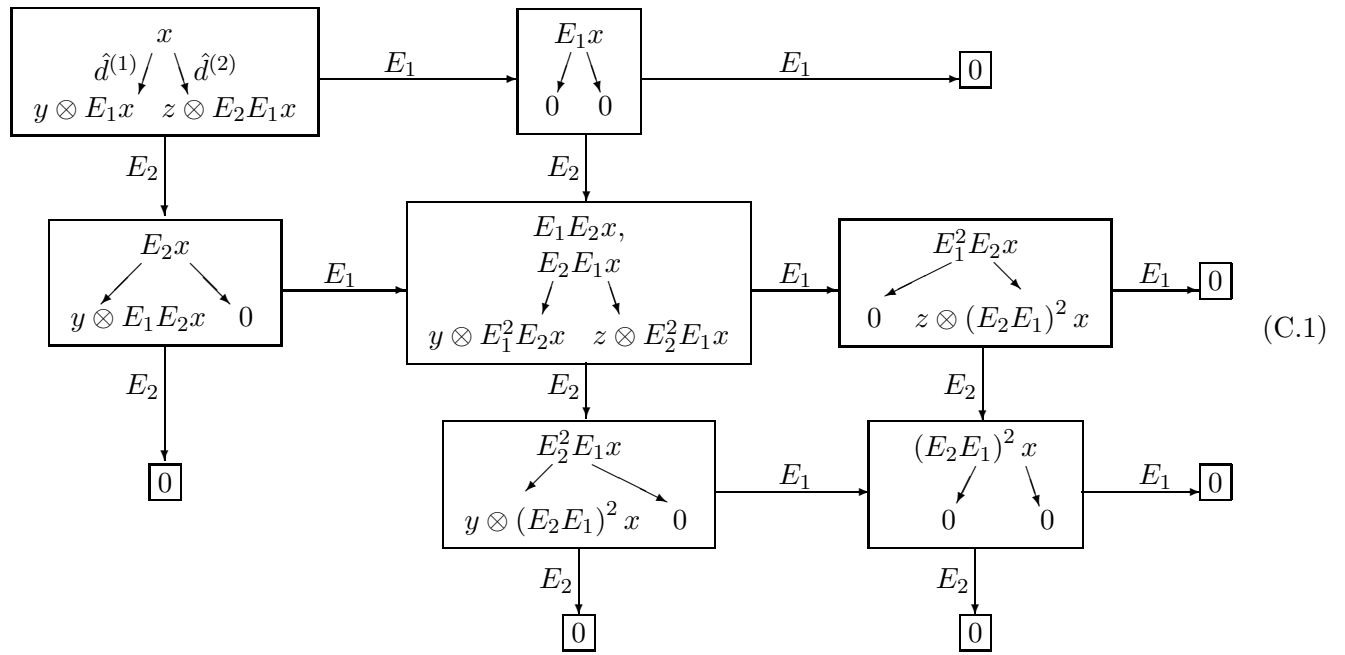
Next, the number of the linearly independent vectors among $\left\{ \hat{d}_{k+1} x_{i,k} \right\}_{i=1}^{\dim \mathcal{V}_k}$ is by definition $\dim \text{Im } \hat{d}_{k+1}$, and because $\hat{d}_{k+1} z_{k,i} = 0$ for all i (thanks the nilpotency condition $\hat{d}_{k+1} \hat{d}_k = 0$), the basis vectors in $\text{Im } \hat{d}_{k+1}$ must be found among the vectors $\hat{d}_{k+1} x_{k,i}$. Take then the

Images of all the remaining basis vectors are expanded as $\hat{d}_{k+1}x_{k,j} = \sum_{i=1}^{\dim \text{Im } \hat{d}_{k+1}} \alpha_i \hat{d}_{k+1}y_{k,i}$ for some α (all vanishing in the particular case $\hat{d}_{k+1}x_{k,l+1} = 0$), so that the vectors $h_{k,i} \equiv x_{k,j} - \sum_{i=1}^{\dim \text{Im } \hat{d}_{k+1}} \alpha_i y_{k,i}$. Indeed, $h_{k,i} \notin \text{Im } \hat{d}_k$ by definition, $\hat{d}_{k+1}h_{k,i} = 0 \Rightarrow h_{k,i} \in \ker \hat{d}_{k+1}$, and these vectors are linearly independent thanks to the first addends.

The basis in the first space \mathcal{V}_0 is chosen just in same way, if assume $\mathcal{V}_{-1} \equiv \emptyset$. Similarly, the latter space \mathcal{V}_n is no longer selected if set $\mathcal{V}_{n+1} \equiv \emptyset$.

C Morphisms of the representation spaces. A more involved example

Here we provide a one more illustration to the discussed in 4 representation theory standpoint on the KhR formalism. The figure below demonstrates a non-trivial (not exact) map of two $[2, 1]$ type representations of the su_3 algebra [38] permitted by the supposed properties of the morphisms.



D List of braids providing the unique level I reminders

E Examples of the unique minimal remainders related to the CohFT diagrams in the case of three strands

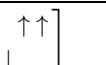
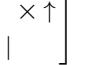
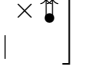
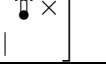
E.1 The doubly twisted diagram of the unknot

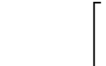
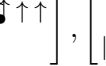
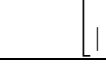
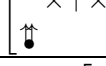
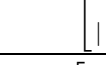
$[1, 2]$, the doubly twisted unknot				
T -grading	q -grading	χ	Diagrams	Khovanov polynomial, q -gradings of the terms
0	$2 + \Delta_{111}$	1		3, 1
	$2 + \Delta_{001}$	1		
	$2 + \Delta_{011}$	1		
	$2 + \Delta_{000}$	1		
1	Δ_{011}	-1		
	Δ_{001}	-1		

E.2 The trefoil knot in different three strand presentations

1. [1112], the Trefoil knot				
T -grading	q -grading	$ \chi $	Diagrams	Khovanov polynomial, q -gradings of the terms
0	$4 + \Delta_{111}$	1		-1, -3
	$4 + \Delta_{000}$	1		
	$4 + \Delta_{001}$	1		
	$4 + \Delta_{011}$	1		
1	$2 + \Delta_{011}$	1		
	$2 + \Delta_{001}$	1		
2	$2 + \Delta_{100}$	1		-5
	$2 + \Delta_{101}$	1		
	Δ_{011}	1		
3	$2 + \Delta_{011}$	1		-9
	Δ_{101}	2		
	Δ_{100}	1		
4	$2 + \Delta_{101}$	1		

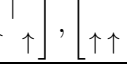
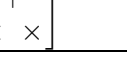
2. [1121], the Trefoil knot				
T -grading	q -grading	$ \chi $	Diagrams	Khovanov polynomial, q -gradings of the terms
0	$4 + \Delta_{111}$	1		-1, -3
	$4 + \Delta_{000}$	1		
	$4 + \Delta_{011}$	1		
	$4 + \Delta_{001}$	1		
1	$2 + \Delta_{001}$	1		
	$2 + \Delta_{011}$	1		
2	$2 + \Delta_{101}$	1		-5
	$2 + \Delta_{010}$	1		
3	Δ_{101}	1		-9
	Δ_{010}	1		

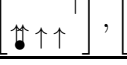
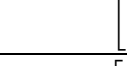
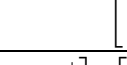
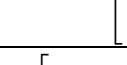
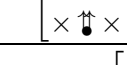
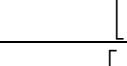
3. [1211], the Trefoil knot				
T -grading	q -grading	$ \chi $	Diagrams	Khovanov polynomial, q -gradings of the terms
0	$4 + \Delta_{001}$	1		-1, -3
	$4 + \Delta_{011}$	1		
	$4 + \Delta_{111}$	1		
	$4 + \Delta_{000}$	1		
1	$2 + \Delta_{001}$	1		
	$2 + \Delta_{011}$	1		
2	$2 + \Delta_{101}$	1		-5
	$2 + \Delta_{010}$	1		
3	Δ_{010}	1		-9
	Δ_{101}	1		

4. [2111], the Trefoil knot				
T -grading	q -grading	$ \chi $	Diagrams	Khovanov polynomial, q -gradings of the terms
0	$4 + \Delta_{111}$	1		-1, -3,
	$4 + \Delta_{000}$	1		
	$4 + \Delta_{011}$	1		
	$4 + \Delta_{001}$	1		
1	$2 + \Delta_{001}$	1		
	$2 + \Delta_{011}$	1		
2	$2 + \Delta_{101}$	1		-5
	Δ_{011}	1		
	$2 + \Delta_{100}$	1		
3	Δ_{100}	1		-9
	Δ_{101}	2		
	$2 + \Delta_{011}$	1		
4	$2 + \Delta_{101}$	1		

5. [1222], the Trefoil knot				
T -grading	q -grading	$ \chi $	Diagrams	Khovanov polynomial, q -gradings of the terms
0	$4 + \Delta_{001}$	1		-1, -3
	$4 + \Delta_{011}$	1		
	$4 + \Delta_{111}$	1		
	$4 + \Delta_{000}$	1		
1	$2 + \Delta_{001}$	1		
	$2 + \Delta_{011}$	1		
2	$2 + \Delta_{110}$	1		-5
	Δ_{001}	1		
	$2 + \Delta_{010}$	1		
3	Δ_{110}	1		-9
	Δ_{010}	2		
	$2 + \Delta_{001}$	1		
4	$2 + \Delta_{010}$	1		

6. [2122], the Trefoil knot				
T -grading	q -grading	$ \chi $	Diagrams	Khovanov polynomial, q -gradings of the terms
0	$4 + \Delta_{111}$	1		-1, -3
	$4 + \Delta_{000}$	1		
	$4 + \Delta_{011}$	1		
	$4 + \Delta_{001}$	1		
1	$2 + \Delta_{001}$	1		
	$2 + \Delta_{011}$	1		
2	$2 + \Delta_{101}$	1		-5
	$2 + \Delta_{010}$	1		
3	Δ_{101}	1		-9
	Δ_{010}	1		

7. [2212], the Trefoil knot				
T -grading	q -grading	$ \chi $	Diagrams	Khovanov polynomial, q -gradings of the terms
0	$4 + \Delta_{001}$	1		-1, -3
	$4 + \Delta_{011}$	1		
	$4 + \Delta_{111}$	1		
	$4 + \Delta_{000}$	1		
1	$2 + \Delta_{001}$	1		-5
	$2 + \Delta_{011}$	1		
2	$2 + \Delta_{101}$	1		-9
	$2 + \Delta_{010}$	1		
3	Δ_{010}	1		-9
	Δ_{101}	1		

8. [2221], the Trefoil knot				
T -grading	q -grading	$ \chi $	Diagrams	Khovanov polynomial, q -gradings of the terms
0	$4 + \Delta_{111}$	1		-1, -3
	$4 + \Delta_{000}$	1		
	$4 + \Delta_{011}$	1		
	$4 + \Delta_{001}$	1		
1	$2 + \Delta_{001}$	1		-5
	$2 + \Delta_{011}$	1		
2	$2 + \Delta_{110}$	1		-9
	$2 + \Delta_{010}$	1		
	Δ_{001}	1		
3	Δ_{110}	1		-9
	Δ_{010}	2		
	$2 + \Delta_{001}$	1		
4	$2 + \Delta_{010}$	1		

9. [1212], the Trefoil knot					10. [2121], the Trefoil knot				
T -grading	q -grading	$ \chi $	Diagrams	Khovanov polynomial, q -gradings of the terms	T -grading	q -grading	$ \chi $	Diagrams	Khovanov polynomial, q -gradings of the terms
0	$4 + \Delta_{111}$	1		-1, -3	0	$4 + \Delta_{001}$	1		-1, -3
	$4 + \Delta_{000}$	1				$4 + \Delta_{011}$	1		
	$4 + \Delta_{011}$	1				$4 + \Delta_{111}$	1		
	$4 + \Delta_{001}$	1				$4 + \Delta_{000}$	1		
1	$2 + \Delta_{001}$	1			1	$2 + \Delta_{001}$	1		
	$2 + \Delta_{011}$	1				$2 + \Delta_{011}$	1		
2	$2 + \Delta_{101}$	1		-5	2	$2 + \Delta_{101}$	1		-5
	$2 + \Delta_{010}$	1				$2 + \Delta_{010}$	1		
3	Δ_{101}	1		-9	3	Δ_{010}	1		-9
	Δ_{010}	1				Δ_{101}	1		

E.3 The “thick” knot 8_{19} (torus $T[3,4]$)

[12122122], knot 8 ₁₉ , or torus $T[3,4]$				
T -gr.	q -gr.	$ \chi $	Diagrams	Kh.pol., q -grds.
0	$8 + \Delta_{000}$	1		5, 7
	$8 + \Delta_{111}$	1		
	$8 + \Delta_{011}$	1		
	$8 + \Delta_{001}$	1		
1	$6 + \Delta_{011}$	1		9
	$6 + \Delta_{001}$	1		
2	$6 + \Delta_{010}$	1		9
	$6 + \Delta_{101}$	1		
3	$4 + \Delta_{010}$	1		13
	$4 + \Delta_{101}$	1		
4	$4 + \Delta_{100}$	1		11, 13
	$2 + \Delta_{001}$	1		
4	$4 + \Delta_{110}$	1		
	$2 + \Delta_{011}$	1		
5	Δ_{001}	1		15, 17
5	$2 + \Delta_{100}$	1		
	$2 + \Delta_{110}$	1		
5	Δ_{011}	1		